Report of Investigations No. 110

STATISTICAL ANALYSIS OF LINEAMENTS AND THEIR RELATION TO FRACTURING, FAULTING, AND HALOKINESIS IN THE EAST TEXAS BASIN

Owen R. Dix and M. P. A. Jackson

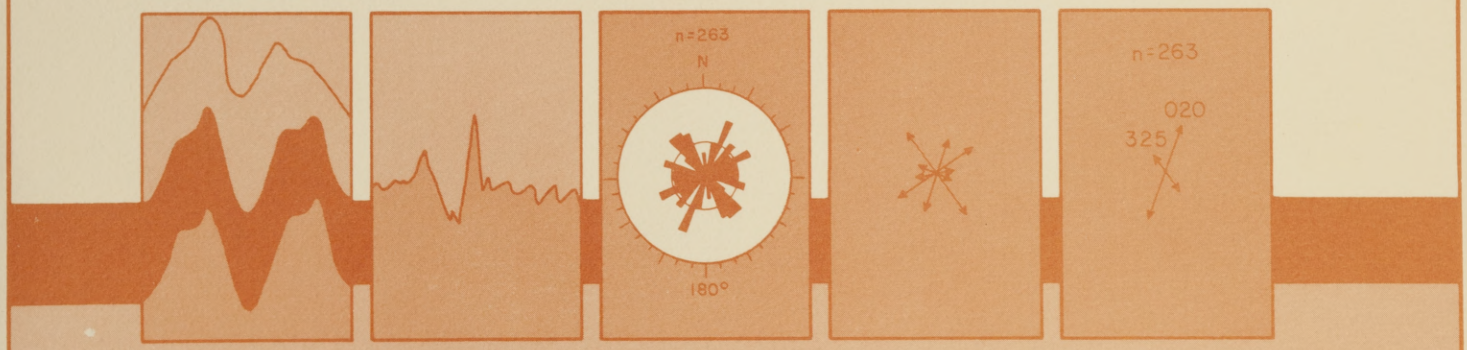

1981
Bureau of Economic Geology
W. L. Fisher, Director
The University of Texas at Austin
Austin, Texas 78712

Report of Investigations No. 110

STATISTICAL ANALYSIS OF LINEAMENTS AND THEIR RELATION TO FRACTURING, FAULTING, AND HALOKINESIS IN THE EAST TEXAS BASIN

Owen R. Dix and M. P. A. Jackson

1981
Bureau of Economic Geology
W. L. Fisher, Director
The University of Texas at Austin
Austin, Texas 78712

Project funded by
the U.S. Department of Energy
Contract Nos. DE-AC97-79ET-44605
and DE-AC97-80ET-46617

CONTENTS

FIGURES

TABLES

ABSTRACT

Lineament analysis is part of a broad spectrum of structural studies employed to determine the tectonic stability of the East Texas Basin. Such information is necessary to assess the suitability of East Texas salt domes as possible repository sites for the storage of high-level nuclear wastes. A sequence of statistical operations was designed to identify and assess the significance of lineament preferred orientation by means of a variety of statistical tests or parameters, including vector summation, length weighting, χ^2, F, and t testing, the Bernshtein accuracy criterion, and an index of preferred orientation. Black-and-white aerial photographs, at scales between 1:17,400 and 1:25,500, and band-5 Landsat imagery were analyzed. Well-defined, northeast-trending and northwest-trending lineament populations are present throughout the East Texas Basin. The northeast trend, comprising two peaks oriented at 045° and 055°, corresponds to the orientation of the Mexia-Talco peripheral fault zone, to subsurface faults in the center of the basin, and to some lithologic contacts. The northwest trend comprises two peaks oriented at 310° and 325°. Both the northeast and northwest trends are thought to result from preferential directions of fracture induced by interference folding at depth. This folding is caused by halokinesis and is reflected in the regional gravity field. The Elkhart - Mount Enterprise fault zone has exerted little noticeable effect on the regional lineament pattern, mainly because of its subparallel orientation. Areas above shallow salt domes, particularly those in the southern part of the basin, are associated with higher lineament densities and lower preferred orientation of lineaments than are non-dome areas or areas above deep salt diapirs; this probably reflects radial and concentric fault and fracture patterns above the shallow domes. Analysis of computer-generated, geologically meaningless sets of "lineaments" strongly suggests that confidence levels of 99 percent are necessary to exclude randomly generated peaks, and that the significance of orthogonal pairsets has been exaggerated in the literature.

INTRODUCTION

Lineaments have been defined as mappable linear or curvilinear surface features that are thought to reflect subsurface phenomena (O'Leary and others, 1976).

This study is part of the Bureau of Economic Geology's East Texas Waste Isolation program, which consists of geologic, hydrologic, geomorphic, and remote-sensing investigations of the East Texas salt dome basin, both on a regional scale and on specific domes. The assessment of salt domes as repositories for high-level nuclear waste storage is the aim of this project. As such, the major considerations are the tectonic and hydrologic stability of the diapirs.

The present study of lineaments on both aerial photographs and Landsat imagery was carried out to determine regional lineament trends and to examine their relationships to the regional tectonic framework. If the East Texas Basin is tectonically unstable, Holocene movement in the form of upward growth or downward collapse of salt domes, or displacement along any of the fault systems around the basin margin may be detectable in the regional lineament pattern.

An additional goal of the present project was to evaluate existing methods of lineament analysis and to develop new methods where necessary.

REGIONAL SETTING

The East Texas area is a structural and depositional basin forming part of the larger East Texas Embayment (fig. 1). The basin is approximately 160 km wide and is bounded by the Elkhart - Mount Enterprise fault zone, the Mexia-Talco fault zone, and the Sabine Uplift (fig. 2). Infilling of the basin by clastics, carbonates, and evaporites began in the Triassic. Sedimentary environments evolved from purely continental, through restricted marine, to open shallow marine. Deposition continued during the next 180 m.y., culminating with the progradation of delta systems, which caused outbuilding of the continental shelf, followed by a series of marine transgressions. Evaporites, chiefly in the form of halite, constitute the Louann Formation near the base of the succession at depths of 3,000 m to 6,000 m. The Louann Salt has undergone extensive deformation as a result of such factors as unequal loading by the overburden, density inversion caused by the higher densities of overlying sediment, and possible thermal convection within the salt at depth. This has led to the formation of salt pillows, spines, and domes, which have moved relatively upward, deforming, and in places piercing, the overlying and surrounding

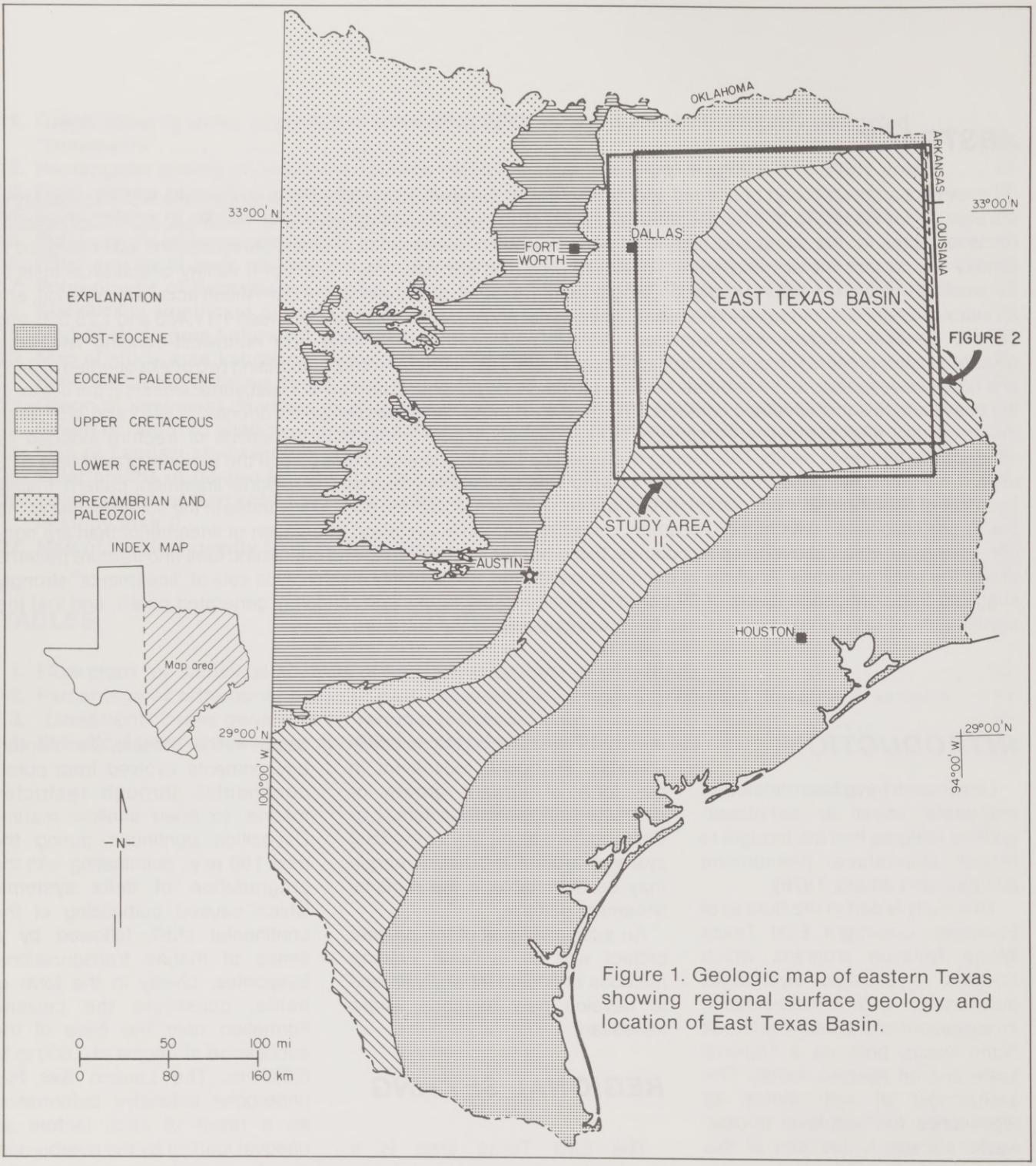

Figure 1. Geologic map of eastern Texas showing regional surface geology and location of East Texas Basin.

strata. Twenty-two salt domes have been identified within the East Texas Basin, ranging in depth from less than 50 m to more than 2,000 m (fig. 3).

The Mexia-Talco fault zone represents a peripheral graben system that developed over the updip limit of the Louann Salt. The grabens extend downward to the Paleozoic basement, the surface of which is planar. The fault zone was active during the Mesozoic and early Tertiary and is likely to be a "pull-apart" structure caused by basinward creep of the post-Louann succession over a décollement layer of Louann Salt (Cloos, 1968). The Elkhart - Mount Enterprise fault system is an irregular zone trending approximately 055° and consisting of an array of en echelon and parallel faults having a mean strike of 065°. The location of the Elkhart -

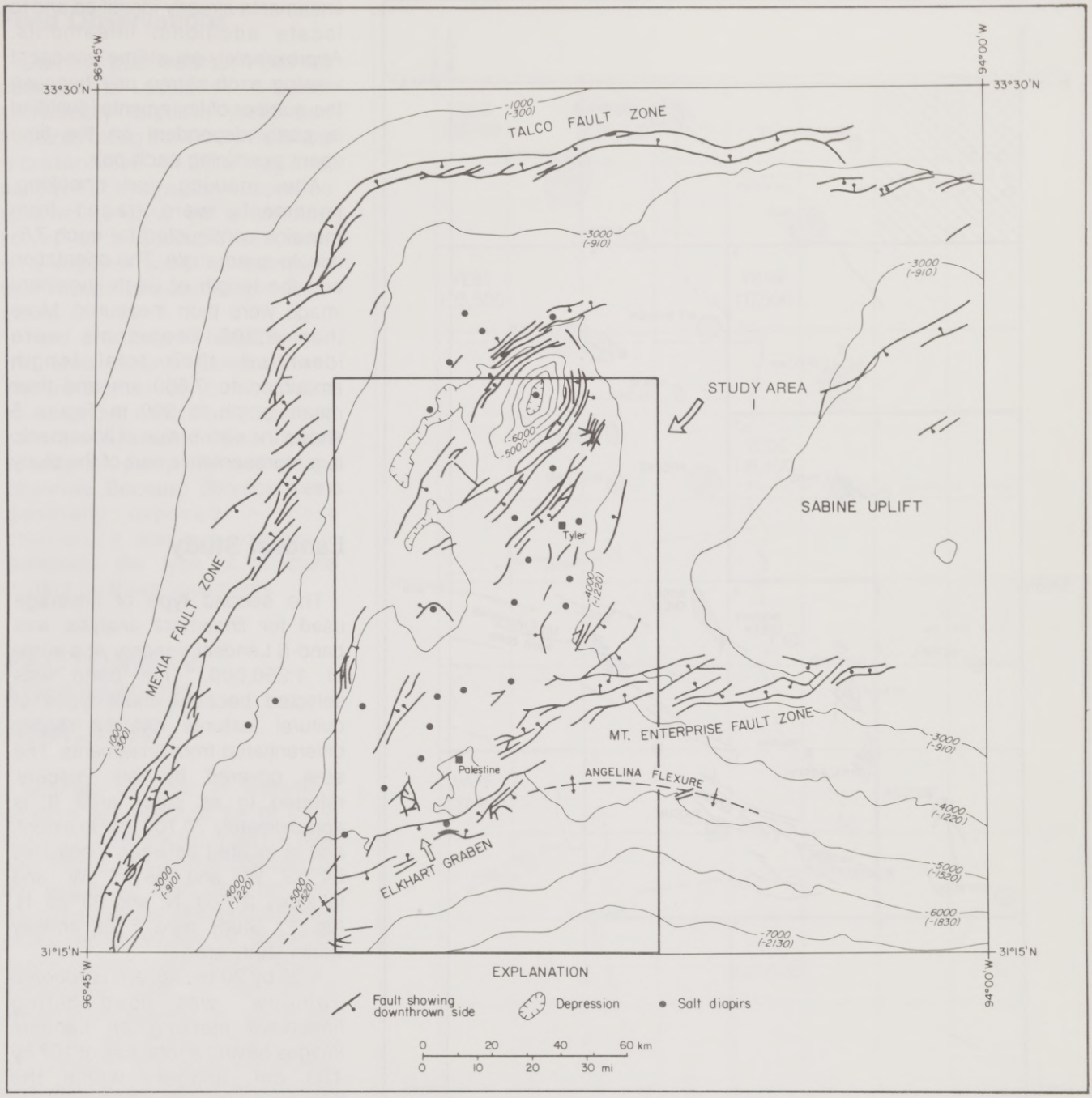

Figure 2. Subsurface structural map of the East Texas Basin showing fault traces and structure contours (in feet and meters below sea level) on the base of the Austin Chalk (published with permission of Geomap, 1979). See figure 1 for location.

Mount Enterprise fault zone over a chain of deep salt domes and swells suggests that these faults are also salt controlled, possibly representing a crestal graben system over the deep uplifts. Some of these faults appear to have been active in the Quaternary Period (Collins and others, 1980).

The topography is characterized by subdued relief with exposures of flat-lying, poorly lithified sediments and surficial deposits. The indigenous vegetation is woodland, approximately half of which has been replaced by pastures or crops.

DATA COLLECTION

Aerial Photographic Study

Black-and-white aerial photographs ranging in scale from 1:17,400 to 1:25,500 were used. The region covered by this study,

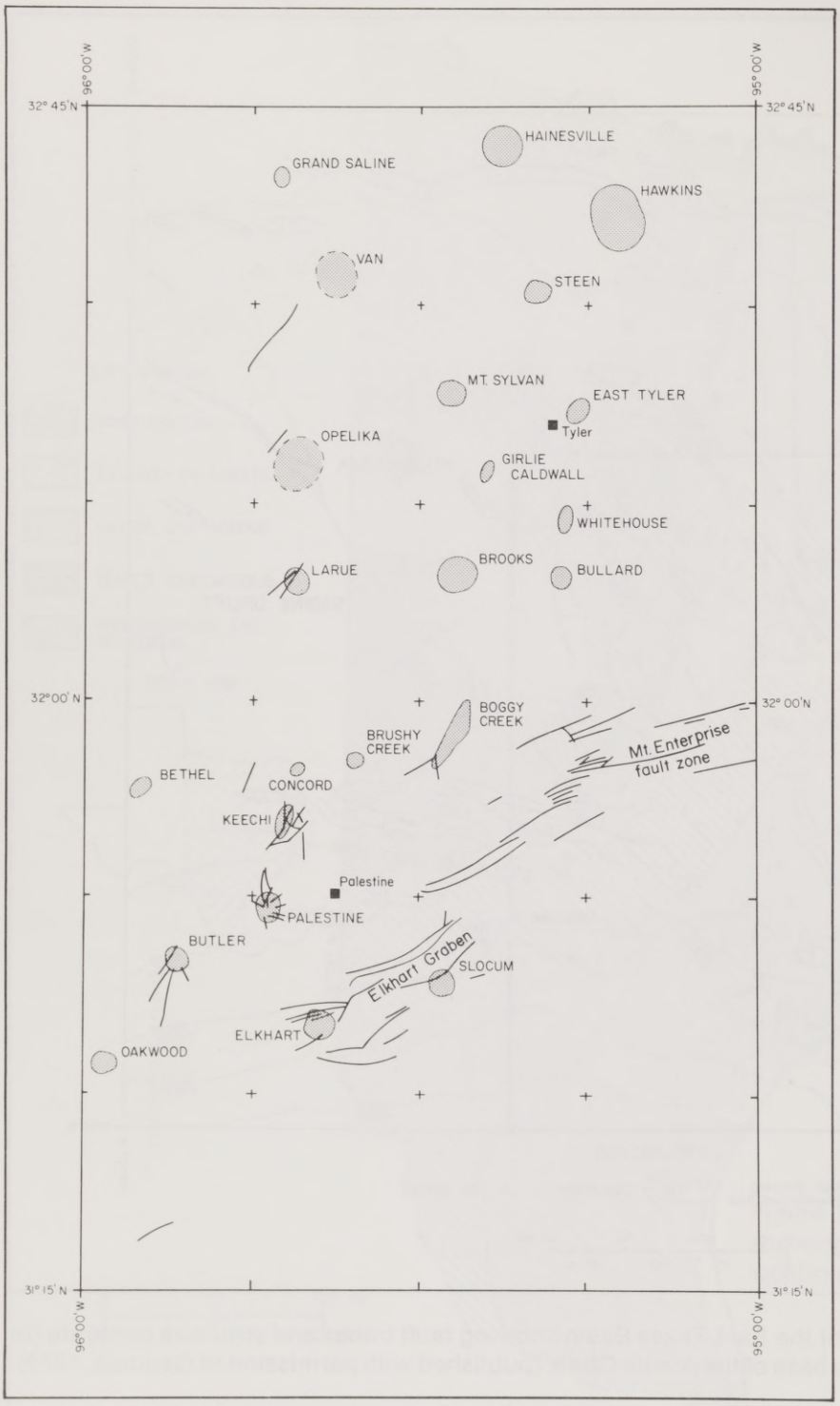

Figure 3. Map of study area I, showing surface fault traces and subsurface diapir configurations. See figure 2 for location.

referred to as study area I, is about 15,400 km^2 in area and lies between longitudes 95°00′ W. and 96°00′ W., and latitudes 31°15′ N. and 32°45′ N. (fig. 3). The area consists of ninety-six 7.5-minute quadrangles; photographic coverage for two quadrangles was unavailable (fig. 4).

Lineaments were identified with the aid of a mirror stereoscope. Each stereo pair was viewed on three separate occasions by two observers in order to check lineaments already identified and to locate additional lineaments. Approximately equal time was spent viewing each stereo pair because the number of lineaments identified is partly dependent on the time spent examining each pair.

After marking and checking, lineaments were traced from mosaics constructed for each 7.5-minute quadrangle. The orientation and the length of each lineament image were then measured. More than 8,300 lineaments were identified; their total length amounted to 7,660 km and their mean length to 900 m. Figure 5 shows the distribution of lineaments in a representative part of the study area.

Landsat Study

The second type of coverage used for lineament analysis was band-5 Landsat imagery at a scale of 1:250,000. This band was selected because most types of cultural features can be readily differentiated from lineaments. The area covered by this imagery, referred to as study area II, is approximately 70,700 km^2 in extent, and is located between longitudes 94°05′ W. and 96°57′ W. and latitudes 31°03′ N. and 33°29′ N. (fig. 1). Study area I lies entirely within study area II.

A 20 by 20 cm square cardboard "window" was used during lineament marking on Landsat images having a total size of 107 by 103 cm. Imagery within the "window" was viewed obliquely in natural light for a set time from eight different angles (that is, the imagery was rotated 45° for each viewing). The "window" was systematically moved over the entire area, allowing 15 percent overlap between successive locations. This ensured uniform viewing over the entire study area. More than 260 lineaments were identified on this imagery. Their lengths ranged from 3 km to 75 km, with a mean length of 10 km.

Field Observations

Owing to poor outcrop, it was not possible to establish whether sporadically exposed joints and fractures along the Trinity River are representative of the regional pattern. For this reason it would be pointless to carry out a selective survey of mesoscopic structures on a regional scale to determine their relation to macroscopic lineaments.

Field checking of lineaments in the area around Oakwood and Keechi Domes by E. W. Collins revealed that more than 70 percent of the lineaments are located entirely or partly along drainage channels. Because bedrock is not generally exposed in these channels, it was not possible to determine the type of structural control on these lineaments.

FACTORS IN LINEAMENT ANALYSIS

Sources of error in lineament analysis are likely to be of three types: (1) *inherent*, such as the type and extent of surficial deposits or the effects of land use; (2) *data handling*, such as effects of different photographic scales or distortion during mosaic construction; and (3) *conceptual*, such as the relative importance allotted to lineament length or frequency, the significance of orthogonal trends, and the selection of meaningful confidence levels to test the significance of lineament peaks. The influence of these factors is discussed below.

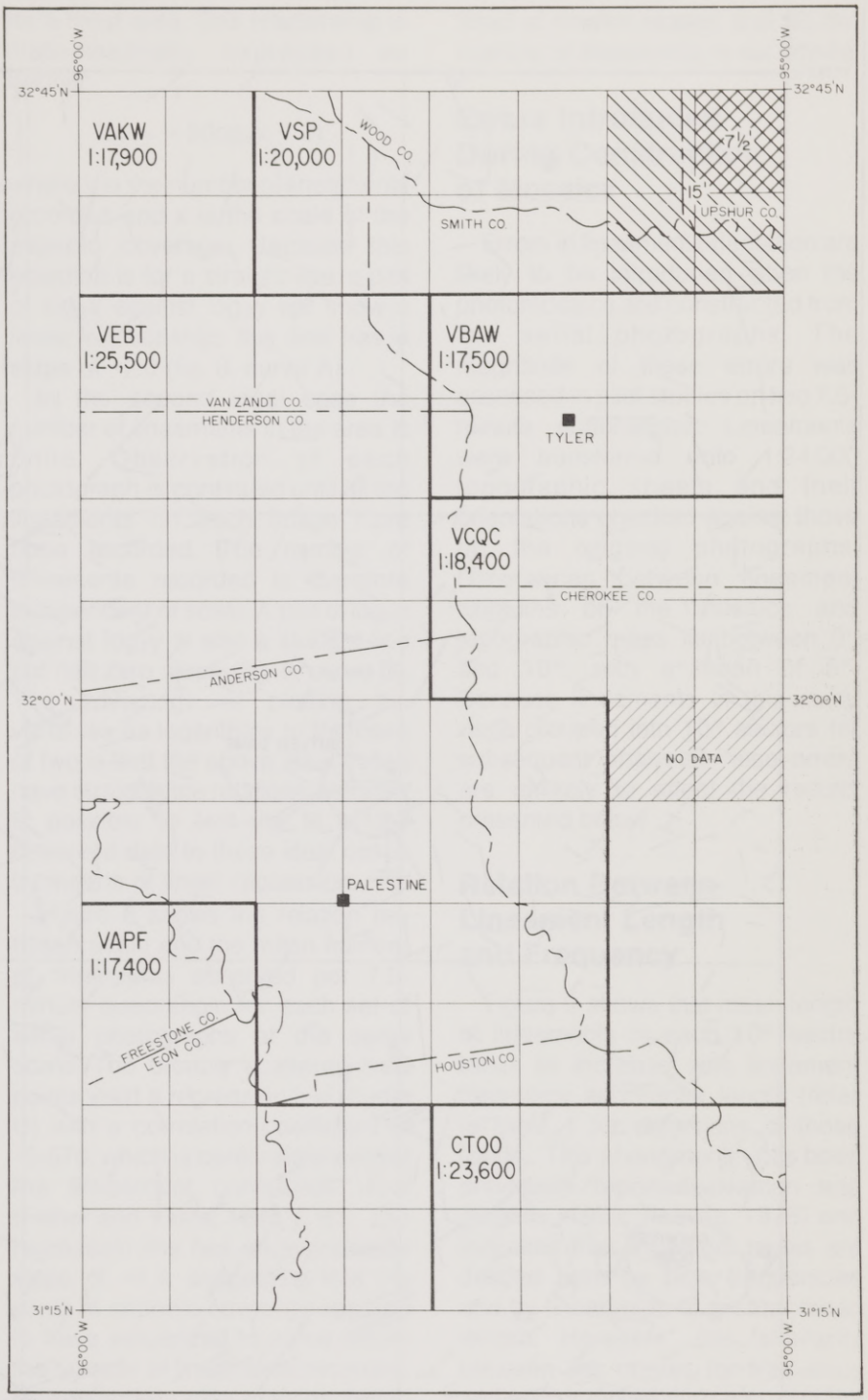

Figure 4. Map of study area I showing aerial photographic coverage and extent of 7.5-minute and 15-minute quadrangles. Letters refer to code for photographic coverage.

Effects of Land Use and Surficial Deposits

In order to evaluate the effects of land use and floodplain deposits on identification of lineaments, the percentage of various terrain parameters was determined for all the quadrangles covered by 1:25,500-scale photography (fig. 4). A 320-point square grid was used on 1:62,500-scale mosaics to determine the proportions of the following land use categories for each of the 36 quadrangles: (1) cities and lakes, (2) pastures and plowed fields, (3) flood plains with pastures, (4) floodplains with indigenous vegetation, and (5) other areas with indigenous vegetation.

A plot of total lineament length versus percentage of indigenous vegetation (categories 4 and 5)

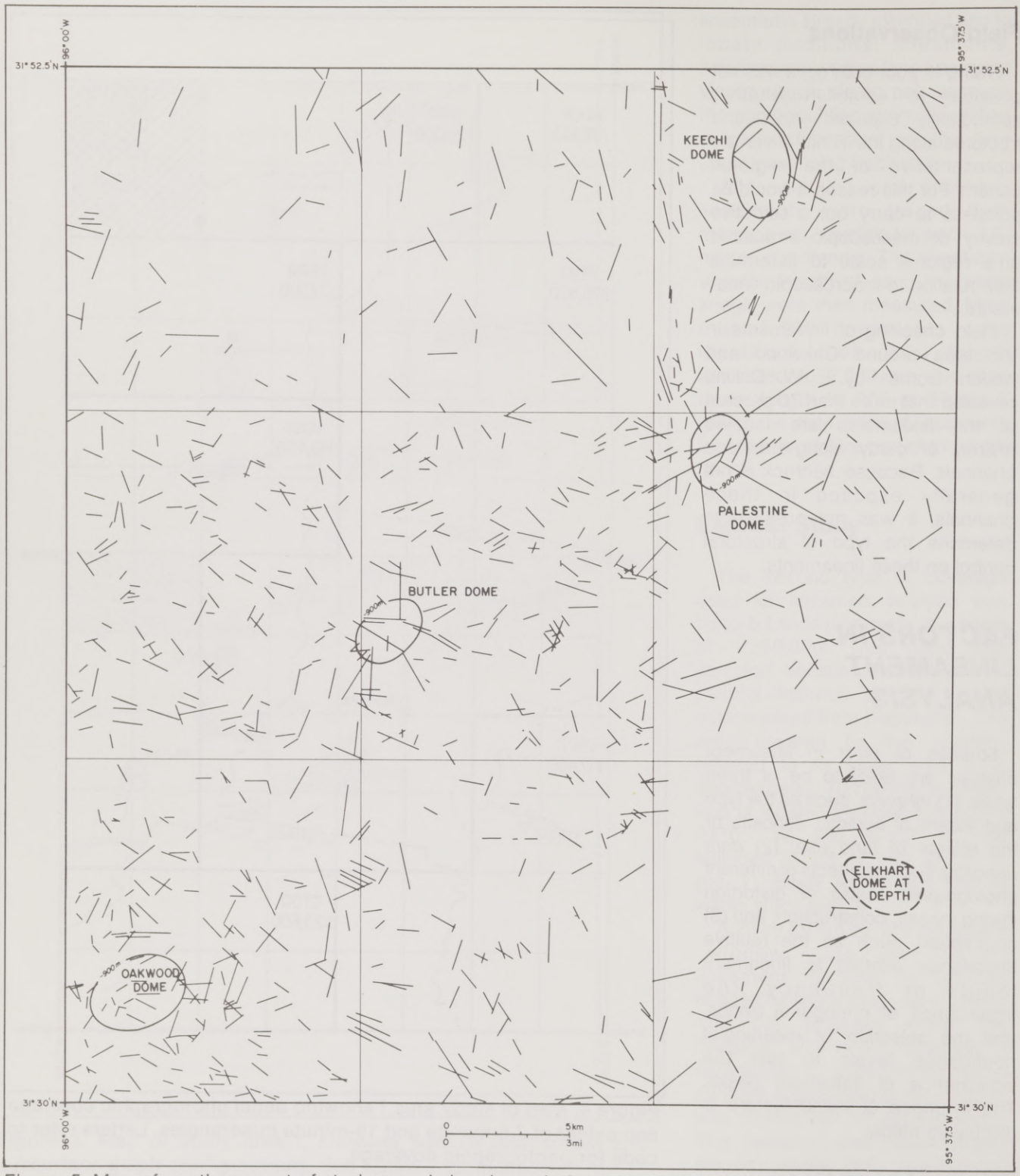

Figure 5. Map of southern part of study area I showing relation between airphoto lineament pattern and salt domes.

reveals a nonsignificant correlation coefficient of +0.171 (fig. 6). This indicates that identification of lineaments was unaffected or only weakly influenced by the presence of pastures and plowed fields. This lack of correlation can possibly be partly accounted for by the high proportion (>70 percent) of lineaments defined by drainage channels, which are generally not obliterated by cultivation.

The negative correlation coefficient between total lineament length in each 7.5-minute quad-

rangle and percentage of area covered by floodplain deposits (categories 3 and 4) is statistically significant at the 95-percent confidence level (fig. 7). This tendency for lower lineament densities to occur in areas covered by surficial deposits has been reported elsewhere. For example, Babcock (1976) postulated that a thicker mantle of surficial deposits would have a greater masking effect on fracture systems in bedrock. This explanation has been questioned on the grounds that areas of anomalously thick glacial drift show a higher-than-average lineament density in places (Haman, 1975), possibly due to differential compaction of the overburden above fractured bedrock (Plafker, 1964).

Effects of Photographic Scale

Because the number of lineaments identified depends partly on the viewing time, approximately equal time was allotted to the study of each photograph. However, the number of photographs covering each quadrangle depends on the scale of the coverage: quadrangles covered by large-scale imagery will have more photographs than quadrangles covered by small-scale imagery. It follows, therefore, that more lineaments will be identified on quadrangles covered by large-scale imagery. The effect of scale on the number of lineaments gathered is best assessed by considering two ideal cases and comparing these with the data of this study.

In the first case we assume that an infinite number of lineaments are present. The number of such lineaments recognized is therefore directly proportional to the time spent examining the area. Where each photograph is examined for a fixed time, as in the present study, the number of lineaments recorded is proportional to the scale because larger scale coverage results in more photographs being examined for a fixed area. This relationship is mathematically expressed as follows:

$$\log_2 y = 2(\log_2 x + 3)$$

where y is the number of lineaments recorded and x is the scale of the airphoto coverage. Because this equation is for a straight line, a plot of $\log_2 x$ against $\log_2 y$ will show a linear relationship; this line has a slope of +2.0 (fig. 8, curve A).

In the second ideal case the number of lineaments in the area is finite. Observation of each photograph is continued until all the lineaments on each image have been recorded. The number of lineaments recorded is therefore independent of scale. A plot of $\log_2 x$ against $\log_2 y$ is also a straight line but has zero slope (fig. 8, curve B). The advantage of plotting the variables as logarithms to the base of two is that the above ideal cases have straight-line relations. Hence it is possible to test the fit of the observed data to these ideal cases by means of linear regression.

Figure 8 shows the relation between scale and the mean number of lineaments observed per 7.5-minute quadrangle for each set of aerial photographs at the same scale. The broadly scattered data points yield a regression line (curve C) with a correlation coefficient of +0.670, which is barely significant at the 90-percent confidence level (Fisher and Yates, 1963, p. 63). The regression line has an appreciable slope of +1.4, suggesting that the scale of airphoto coverage appears to have influenced to some extent the number of lineaments recorded. However, the rather low correlation coefficient indicates that in the present case this relationship cannot be proven at a statistically meaningful confidence level of 95 percent, possibly because of the limited range of scales (1:17,400 to 1:25,500). Two factors may account for the reduced slope of the regression line, as compared with the ideal curve A: (1) megascopic features such as lineaments are better defined at smaller scales, and (2) the number of lineaments is not infinite.

Errors Introduced During Construction of Mosaics

Errors in lineament orientation are likely to be introduced when the photomosaics are constructed from the aerial photographs. The magnitude of these errors was assessed in pilot studies on two 7.5-minute quadrangles. Lineaments were transferred onto 1:24,000 topographic sheets and their orientations checked against those on the original photographs. Differences between lineament azimuths on the mosaics and topographic maps lie between 0° and 10°, with a mean of 5°. Because lineaments in this study were grouped into 10° sectors for subsequent analysis, these errors are unlikely to affect the results presented below.

Relation Between Lineament Length and Frequency

Figure 9 shows that mean length of lineaments in each 10° sector tends to increase with lineament frequency and sector length (refer to table 1 for definitions of these terms). This phenomenon has been previously reported (Haman and Jurgens, 1976; Reeves, 1976) and indicates that lineament peaks are defined both by high frequencies and by lineaments of greater mean length. However, the similarity between the curves for frequency and sector length suggests that the size of a peak (sector length) is more a function of the number of lineaments forming it than of the size of these lineaments.

Randomly Generated "Lineaments"

Artificial data sets were generated by means of random numbers to assess the statistical

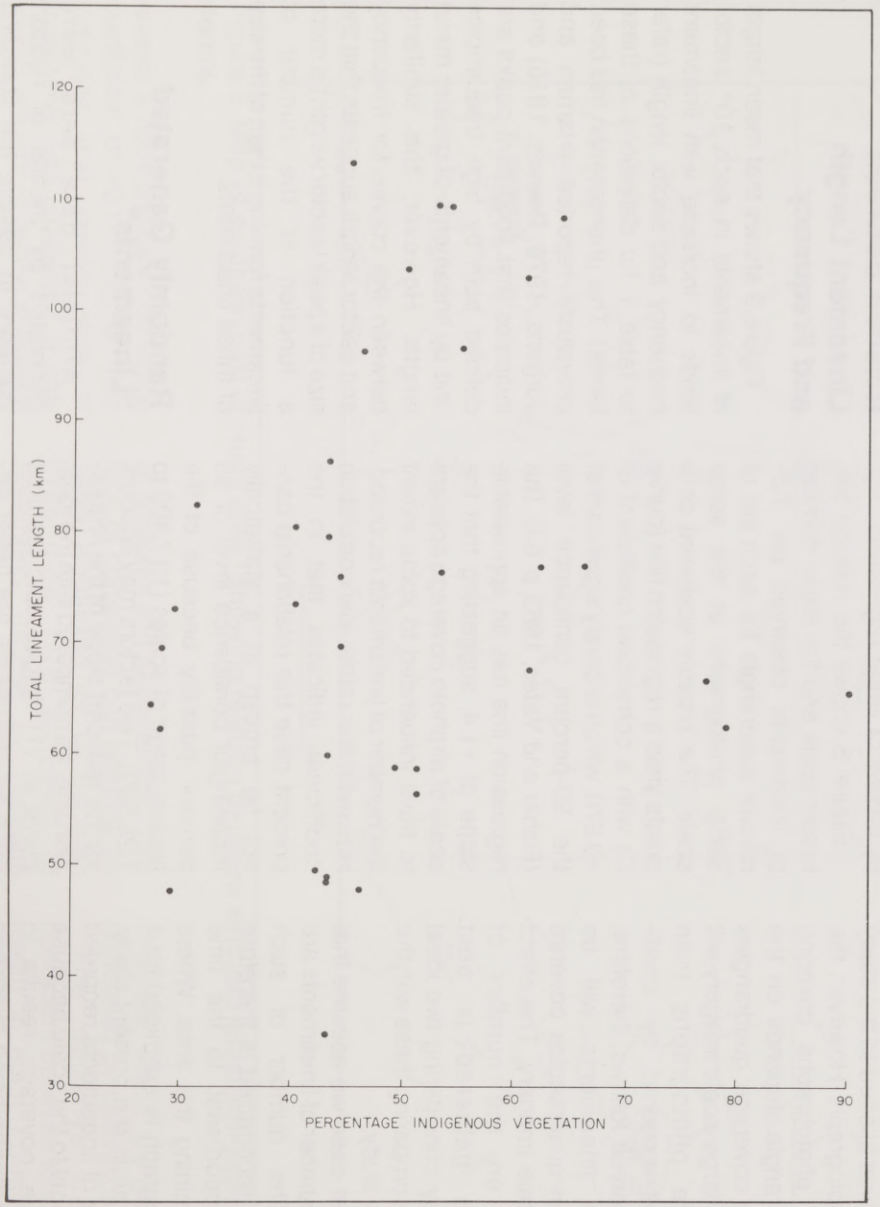

Figure 6. Graph showing lack of correlation between total lineament length (L_T) per 7.5-minute quadrangle (1:25,500-scale coverage) and percentage area covered by indigenous vegetation.

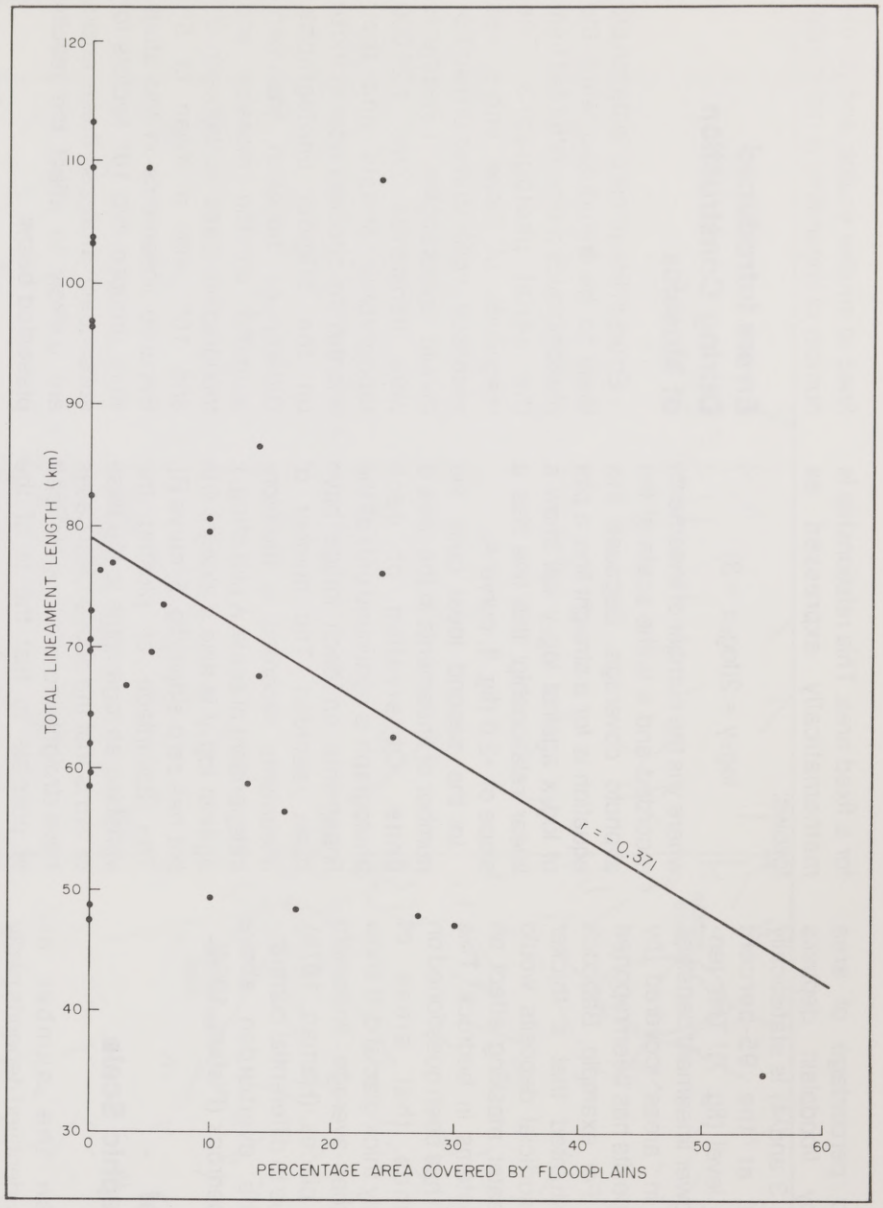

Figure 7. Graph showing significant correlation (at 95-percent level) between total lineament length (L_T) per 7.5-minute quadrangle and percentage area covered by floodplains. See table 1 for explanation of r.

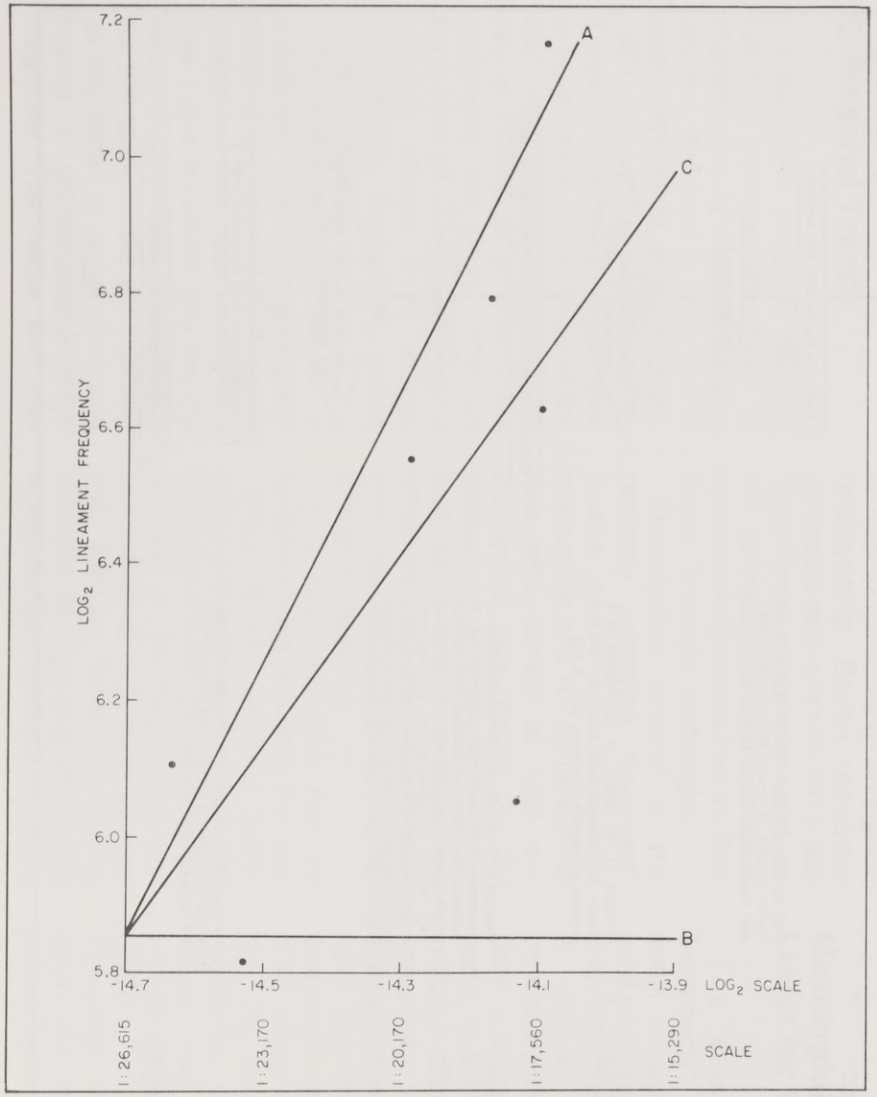

Figure 8. Graph showing effect of aerial photographic scale on numbers of lineaments recognized in each 7.5-minute quadrangle. Each point represents mean number of lineaments per quadrangle for each photographic scale. Curve A: assumes infinite number of lineaments are present, with recognition proportional to observation time. Curve B: assumes finite number of lineaments and total recognition independent of observation time. Curve C: best-fit regression line for actual data.

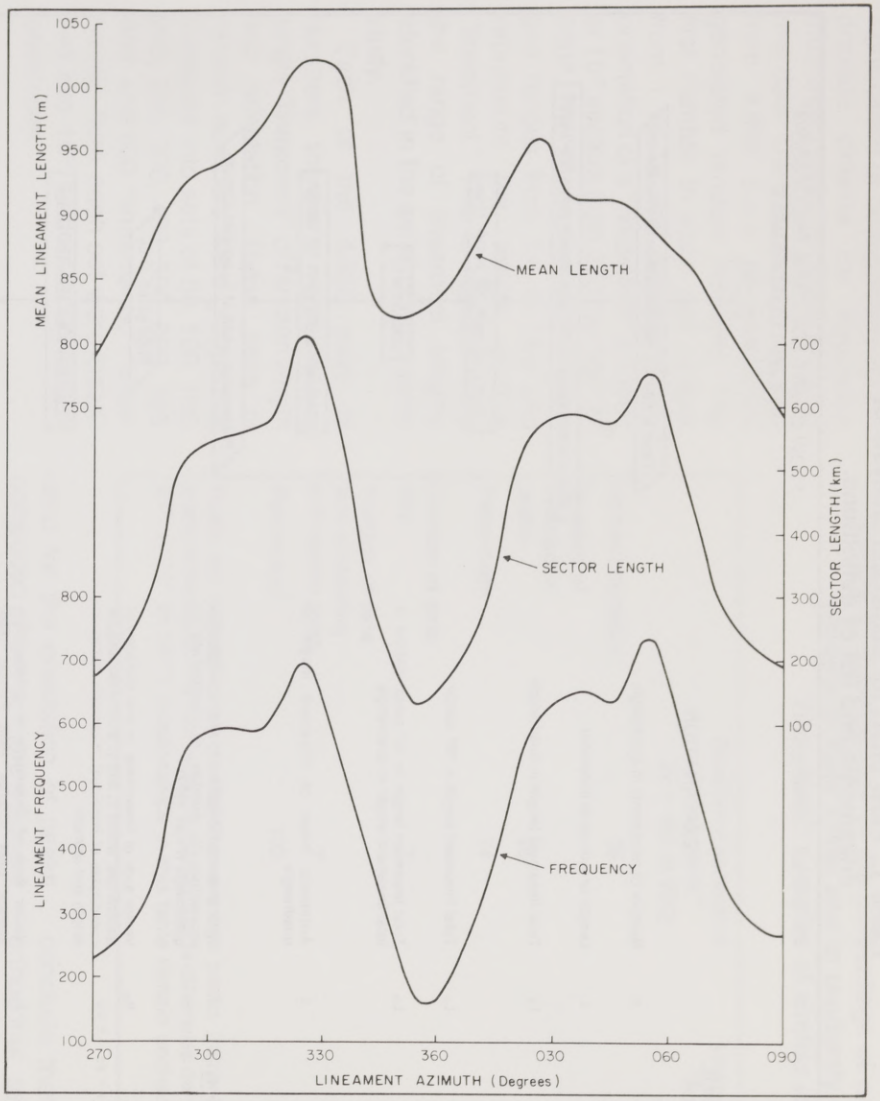

Figure 9. Graph showing relation between mean length, sector length, and frequency of lineaments for study area I (see table 1 for explanation of terms).

Table 1. Flow chart for statistical analysis of lineaments and list of definitions.

TERM, SYMBOL, & FORMULA		EXPLANATION
	n	Number of lineaments in quadrangle
	L	Length of individual lineament
Total length $L_T = \sum_{i=1}^{n} L$	L_T	Total lineament length in quadrangle
Sector length	L_S	Total lineament length in 10° sector
Relative length $L_R = \frac{L_S}{L_T}$	L_R	Total lineament length in 10° sector relative to total lineament length in quadrangle
Mean length $\bar{L} = \frac{L_T}{18}$	$\bar{L}$	Arithmetic mean of lineament length in quadrangle
Length-weighted frequency $F = \frac{L_S \cdot n}{L_T}$	F	Total lineament length in 10° sector, weighted in proportion to number of lineaments in quadrangle (Frost, 1977)
Quadrant vector sum $R_Q = (x_1 + x_2 \ldots + x_n, y_1 + y_2 \ldots + y_n)$	R_Q	Vector sum of lineaments in one quadrant of quadrangle, where x_n and y_n are the rectangular coordinates of individual lineaments based on length and azimuth
Peak vector sum	R_P	Vector sum of lineaments in greater-than-average peak (Curray, 1956; Pincus, 1956) composed of k contiguous 10° sectors whose sector lengths (L_S) exceed the mean length ($\bar{L}$)
Greater-than-average peak $> \bar{L}$	P	
Chi square $\chi^2 = \sum_{i=1}^{k} \frac{(L_S - \bar{L})^2}{\bar{L}}$	χ^2	Test to determine goodness of fit of observed sector lengths in greater-than-average peaks with mean length (Siegel, 1956, p. 42)
Bernshtein accuracy criterion $H = \frac{\chi^2}{\nu}$	H	Measure of the degree of significance of a greater-than-average peak, where $\nu = k - 1 =$ degrees of freedom (Vistelius, 1966, p. 53)
Index of preferred orientation $IPO = \frac{\sum_{i=1}^{18} \lvert L_R - 0.05\bar{5} \rvert \times 100}{1.8\bar{8}}$		Measure of the degree of preferred orientation of lineaments in a quadrangle. Obtained by (1) summing the differences between mean relative length (always $^1/_{18}$ or $0.05\bar{5}$) and relative lengths in each sector; (2) dividing sum by maximum possible value of this parameter; (3) multiplying by 100. Range of IPO is 0% (no preferred orientation) to 100% (perfect unimodal distribution)
Correlation coefficient $r = \frac{\sum_{i=1}^{n} (x_i - \bar{x})(y_i - \bar{y})}{\left[\sum_{i=1}^{n} (x_i - \bar{x})^2 \cdot \sum_{i=1}^{n} (y_i - \bar{y})^2\right]^{1/2}}$	r	Measure of the degree of correlation between any two variables, x and y. Limits of r are -1 and +1 (Gellert and others, 1977)

FLOW CHART FOR DATA PROCESSING IN EACH QUADRANGLE

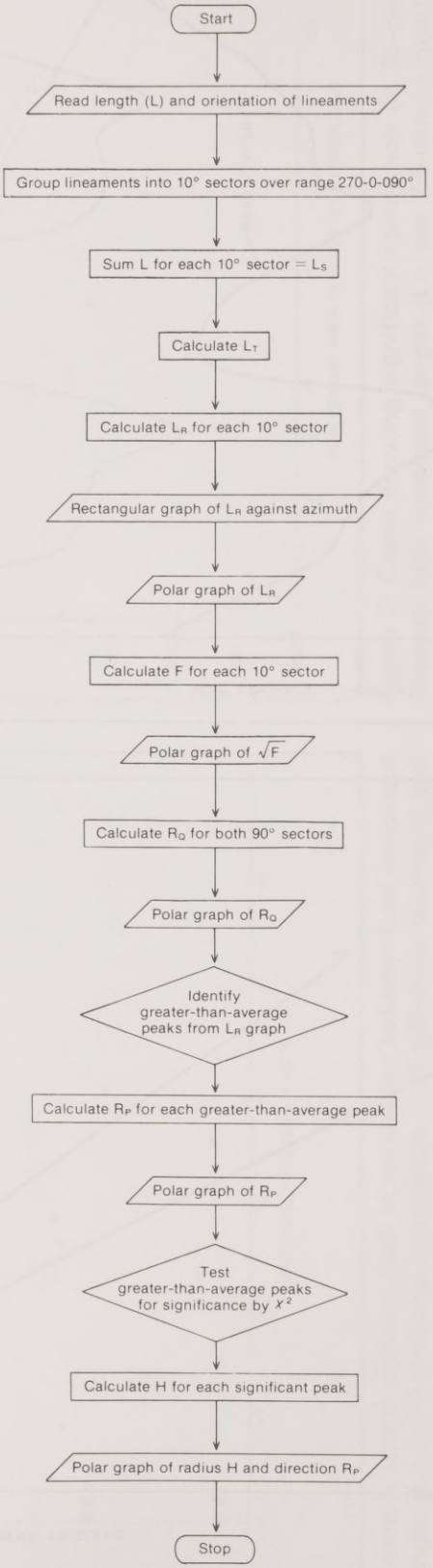

significance of orthogonality and to provide criteria for selecting meaningful levels of significance for real data. The data set was derived from 4,950 pairs of computer-generated random numbers. The first number in each pair ranges from 1 to 18 and represents the orientation of a "lineament" in terms of 10° sectors from 270° to 360° to 090°. The second number in each pair ranges from 1.0 to 15.0 and represents the length of the "lineament." This is approximately the range of lineament lengths identified in the aerial photographic study.

Each of the 4,950 pairs of numbers, therefore, represents a single "lineament" of random length and orientation. These pairs of random numbers were grouped by computer into sets of 50, 100, 150, 200, 250, 300, 400, 500, 600, 700, 800, and 900 "lineaments;" "lineaments" from each set were classified into 10° sectors according to orientation.

Significance of Orthogonal Trends

It has been proposed that the Earth's continental crust is characterized by regional fracture systems that tend to form one or more orthogonal pairsets (Hast, 1973; Gay, 1973; Corbett, 1979). These pairsets have been attributed to (1) changes in the shape of the Earth resulting from variations in the rate of rotation or position of the geographic pole (Kvet, 1976), (2) Earth tides (Rumsey, 1971), or (3) residual effects from tensile stresses in lithospheric plates (Corbett, 1979).

To determine whether a statistically significant orthogonal relationship exists in East Texas, a comparison was made between the East Texas lineament data and the randomly generated "lineaments." For this study, peaks were defined as any sector or group of sectors having a greater-than-average magnitude. The vector sum was used for the orientation of peaks composed of two or more adjacent sectors. A range of 80° to 100° was allowed to constitute an orthogonal relationship. Seven randomly generated data sets with 150 to 600 "lineaments" each were used, as this corresponds with the range in lineament frequencies from the East Texas 15-minute quadrangles.

Seventy-four percent of the randomly generated "lineament" peaks show an orthogonal relationship, and 100 percent of the data sets contain at least one orthogonal pair (table 2). By comparison, only 53 percent of the East Texas lineament peaks are orthogonal, and only 71 percent of those data sets contain at least one orthogonal pair.

It is clear, therefore, that the lineament data sets from the East Texas Basin contain fewer orthogonal pairsets than can be expected to arise purely by chance. In view of the surprisingly high percentage of orthogonal pairsets that can be formed by purely random ordering in data sets having a wide range of sample sizes, we conclude that the significance of orthogonal pairsets has probably been exaggerated in the literature.

Table 2. Comparison of the percentage of orthogonal peaks present in East Texas and in randomly generated "lineament" samples of similar size.

	Randomly generated "lineaments" (n = 150 to 600)	Lineaments from East Texas 15-minute quadrangles (n = 181 to 612)
Number of peaks	35	64
Number of orthogonal peaks	26	34
Percentage	74	53
Number of data sets	7	24
Number of data sets containing orthogonal pairs	7	17
Percentage	100	71

Peaks are defined as all greater-than-average peaks (table 1). Orthogonal refers to peaks oriented 80° to 100° apart; if orthogonal is otherwise defined (for example, 85° to 95°, or 75° to 105°), relationships in this table remain unchanged.

Meaningful Significance Levels for Peaks

The computer-generated "lineaments" also indicate what levels of significance should be used when applying statistical tests to the East Texas data. Polar graphs of relative frequency for the computer-generated "lineaments" show a change from well-defined peaks in small samples to more-uniform distributions in larger samples. Figure 10 shows representative examples of this trend. This change is well displayed by the index of preferred orientation (IPO) values (table 1) of each set (fig. 11), which have a negative logarithmic distribution. The IPO values drop sharply from 100 percent for one "lineament" to 11 percent for 200 "lineaments." Thereafter the decrease is very slight, and the IPO declines to 2 percent for 4,950 lineaments. This

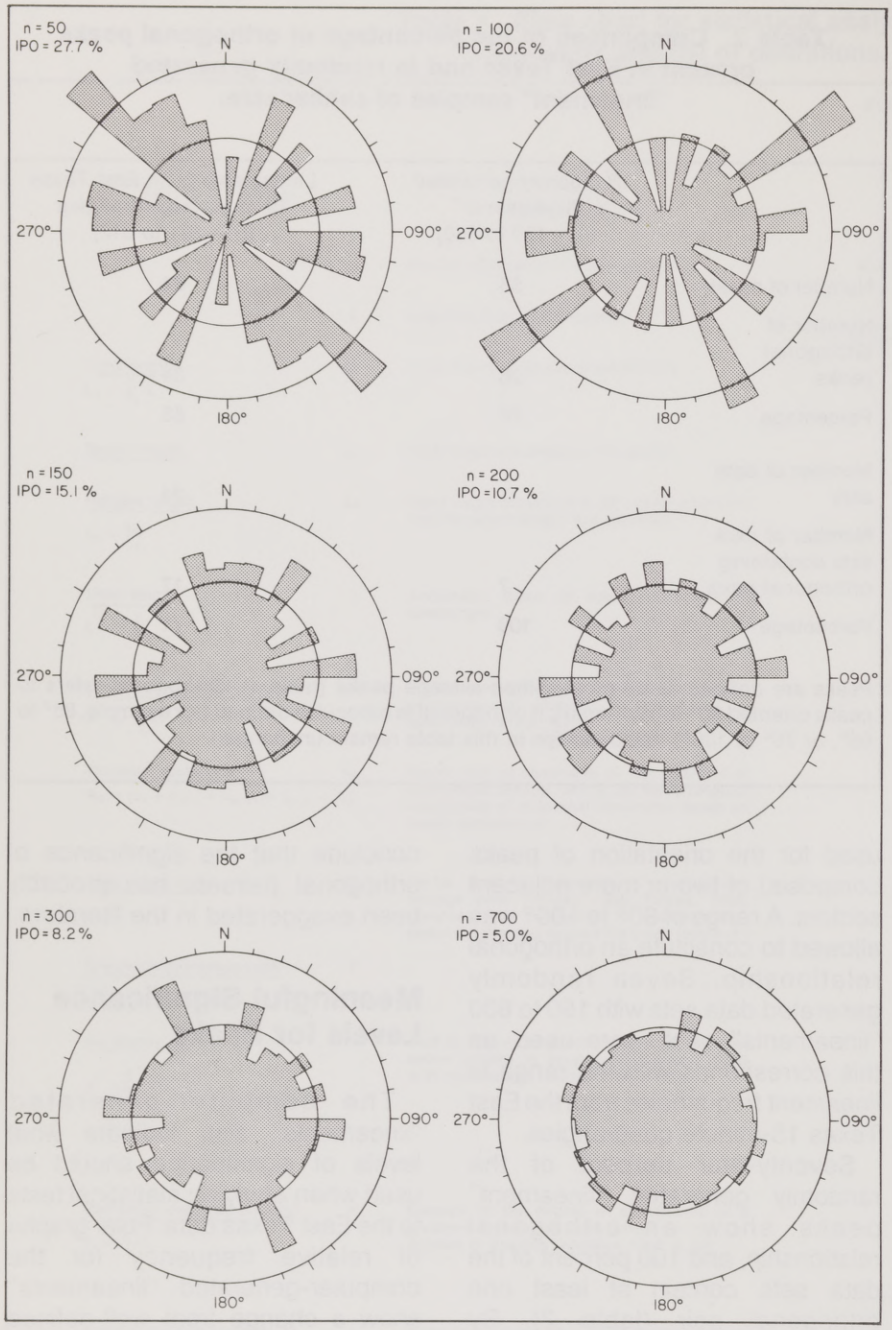

Figure 10. Polar graphs showing square roots of length-weighted frequencies ($\sqrt{F}$) for randomly generated "lineament" populations. Inner circle represents arithmetic mean. Note progressive decrease in IPO with increasing sample size (see table 1 for explanation of F and IPO).

indicates that data sets should contain at least 200 lineaments in order to minimize the effects of randomly oriented lineaments on geologically significant trends.

The X^2 one-sample test was applied to the length-weighted frequencies of greater-than-average peaks (table 1). This revealed that 6 of the 12 data sets have statistically significant peaks at the 95-percent confidence level (table 3). However, none of the sets with more than 100 "lineaments" have significant peaks at the 99-percent confidence level. This level of significance is therefore geologically meaningful, whereas lower levels, commonly applied in the literature, are not. Although peaks that are significant at the 99-percent confidence level can be produced randomly in samples of 100 or less, the 99.9-percent confidence level has not been used because of the danger of committing a type I error, that is, erroneously rejecting meaningful peaks through unrealistically high confidence levels (Davis, 1973, p. 90; Till, 1974, p. 63).

DATA PROCESSING AND RESULTS OF AERIAL PHOTOGRAPHIC STUDY

The lengths and orientations of lineaments in each quadrangle were processed in order to identify preferred orientations (peaks) and to test whether these peaks are statistically significant and, therefore, geologically meaningful. Table 1 contains a simple flow chart of the procedure for data processing.

Rectangular Graphs

Rectangular graphs of relative length versus azimuth have the advantage of facilitating comparisons between peaks of all orientations within different quadrangles (fig. 12). Comparison of peak orientations can best be made between quadrangles along north-south lines of the figure, whereas comparison of relative lengths of peaks can best be made between quadrangles along east-west lines. However, these comparisons are obviously somewhat contrived. Gay (1976) claimed that rectangular graphs of this type allow better definition (to the nearest 1°) of individual peaks than do polar graphs, but precision of this type is a function of the range

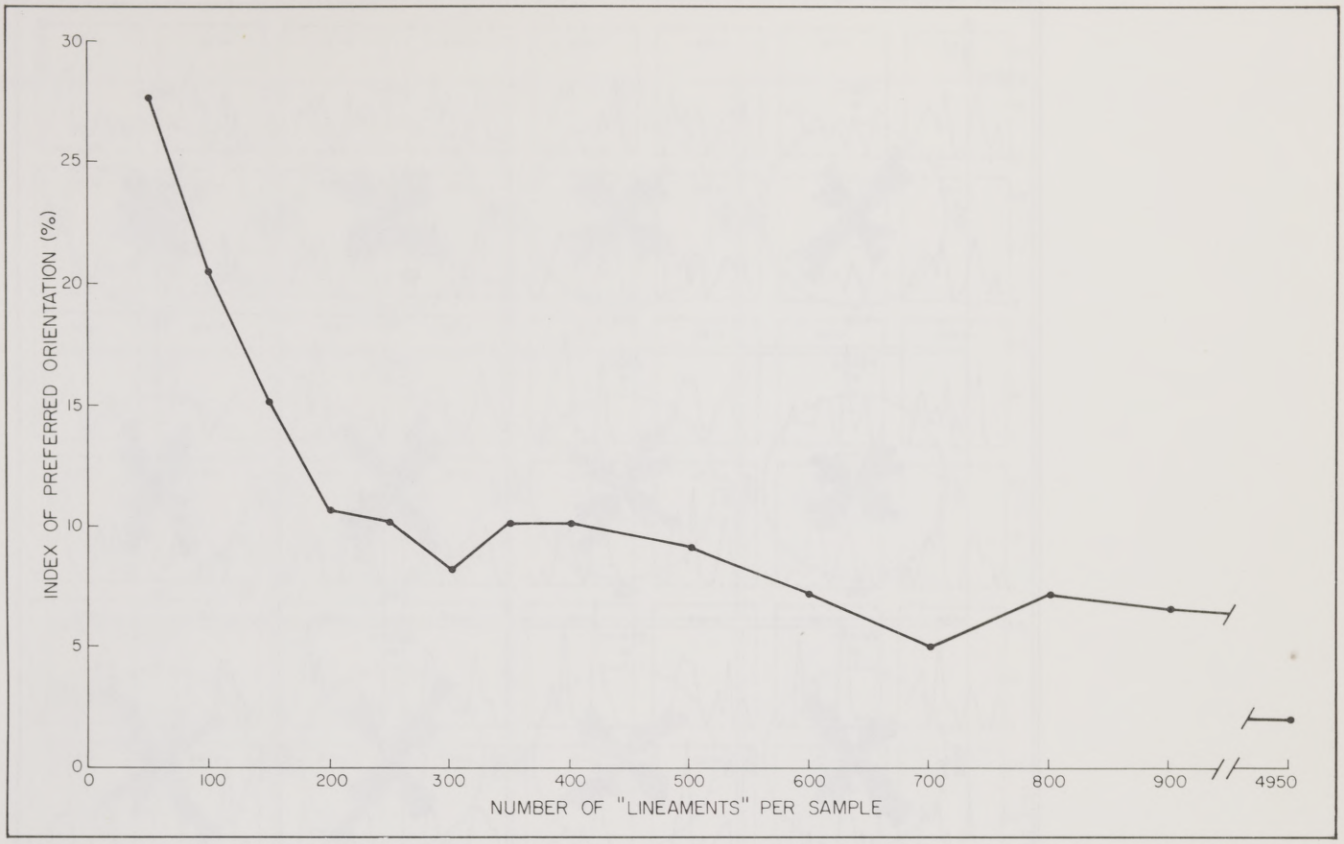

Figure 11. Graph showing relation between index of preferred orientation (IPO) and size of randomly generated "lineament" samples.

of the classes in which the data are grouped and is independent of whether these classes are plotted in a rectangular or polar graph. The rectangular graph has significant advantages over most polar graphs because the area enclosed within the curve of a polar graph increases in proportion to the square of the frequency or length; this tends to exaggerate the importance of peaks (Vistelius, 1966, p. 51). Perhaps the major disadvantage of rectangular graphs is a perceptual one: it is very difficult to visualize directions, even with reference to the abscissa. Because of the clarity and familiarity of polar diagrams, the data are generally presented in this form (table 1).

Polar Graphs

Because long lineaments can be considered as combinations of shorter lineaments (Offield, 1975; Frost, 1977), the combined length of lineaments in each 10° sector (sector length, table 1) is the most accurate measurement of lineament intensity, as this figure is based on both lineament length and frequency.

Comparison of orientation distributions between quadrangles containing different total lengths of lineaments is made easier by normalizing the total length to 1.0, so that the area enclosed by each distribution curve is constant. Sector lengths are thereby converted to relative lengths (table 1). Polar graphs of relative lineament lengths are given in figure 13. However, this type of plot is unsuitable for comparison of lineament intensities in different quadrangles because it obscures the frequencies and lengths of lineaments (Frost, 1977). For this purpose a polar plot of length-weighted frequencies (F in table 1) is used, which has the same shape as polar graphs of relative lineament length, but has a size proportional to lineament total length (fig. 14). As a further refinement, the square root of F is plotted because the area

Table 3. "Lineament" peaks generated by random processes.

Number of "lineaments" in sample	Number of greater-than-average peaks at various significance levels		
	90%	95%	99%
50	1	1	
100	1	1	1
150			
200			
250	1		
300	1	1	
400	1		
500	2	1	
600	1	1	
700			
800	1		
900	2	1	

Figure 12. Rectangular graphs showing relation between lineament azimuth and relative lineament length (L_R) in each 7.5-minute quadrangle in study area I.

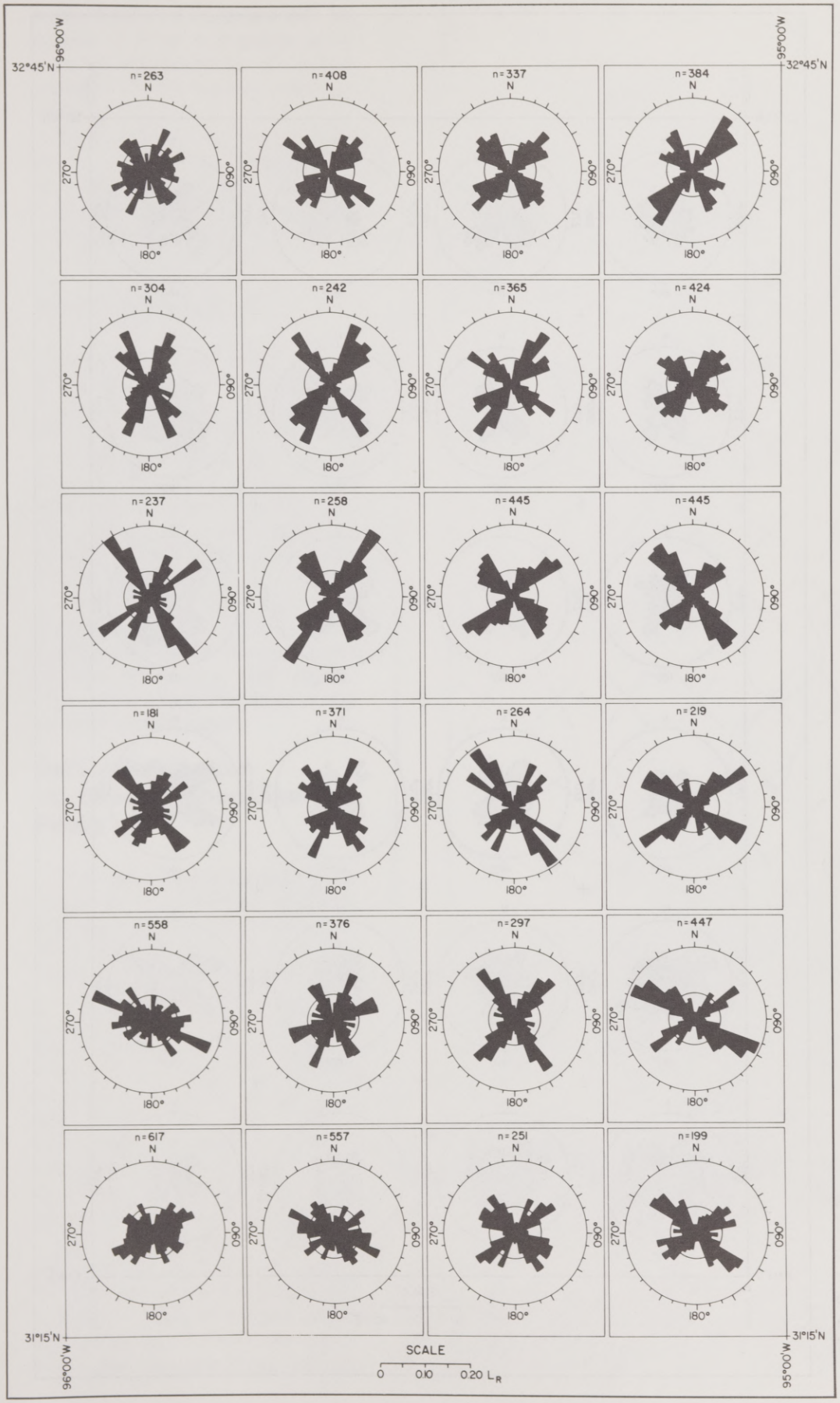

Figure 13. Polar graphs showing relative lengths (L_R) of lineaments in each 15-minute quadrangle in study area I. Inner circle represents arithmetic mean.

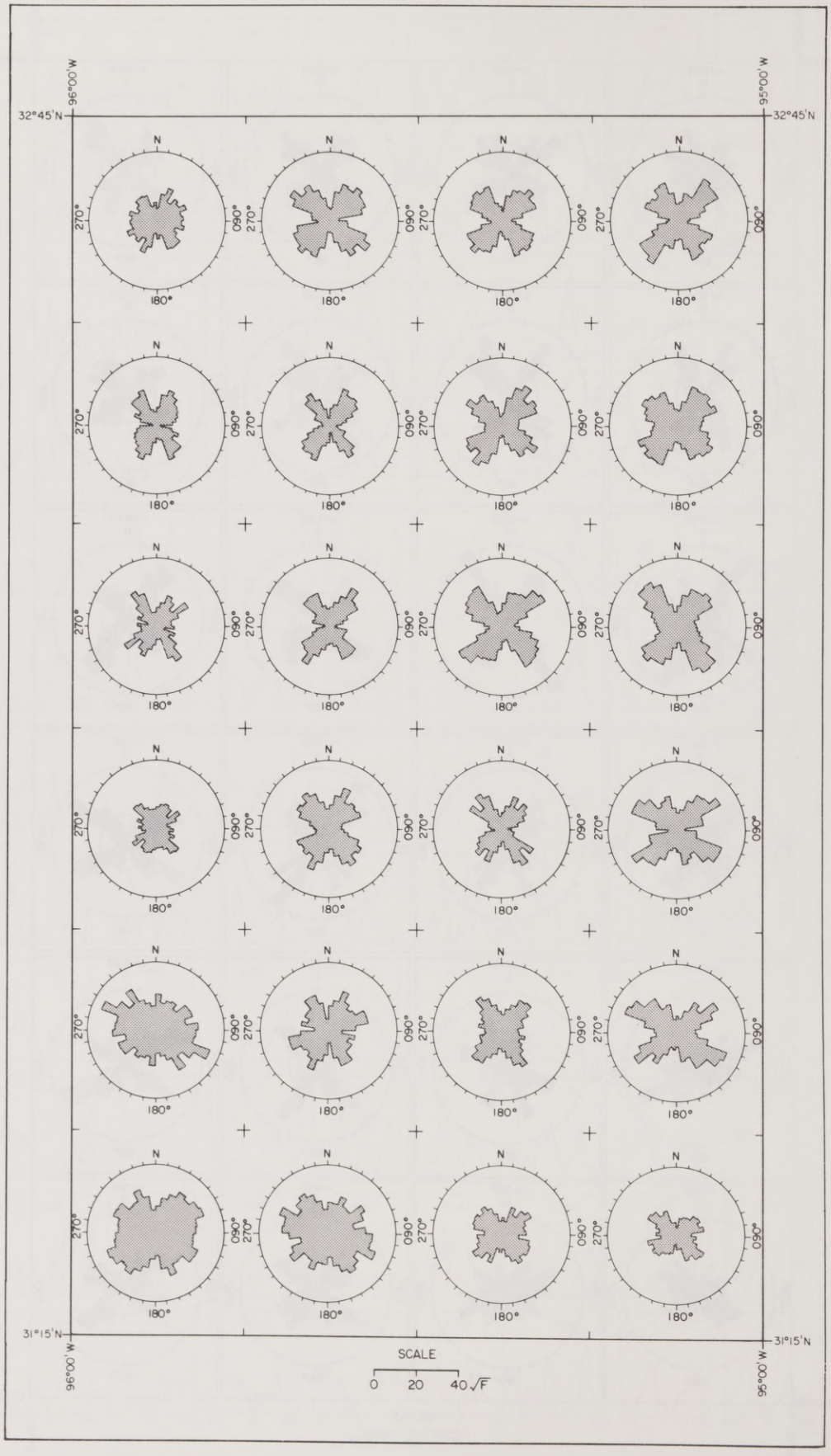

Figure 14. Polar graphs showing square roots of length-weighted frequencies ($\sqrt{F}$) of lineaments in each 15-minute quadrangle in study area I. See figure 13 for sizes of data samples.

under the curve increases with the square of F, so that peaks would become exaggerated in size unless modified in this manner (Vistelius, 1966, p. 51).

Polar plots in figures 13 and 14 reveal distributions ranging from strongly bimodal, with two well-developed peaks, to more-uniform distributions, exhibiting no strong peaks.

Vector Summation

To better define the magnitude and orientation of the prominent trends, two vector sums (one for the northwest quadrant and one for the northeast quadrant) were calculated for both 7.5-minute quadrangles and 15-minute quadrangles (fig. 15). These reveal relatively consistent trends within the ranges of 315° to 330° and 035° to 050°.

The Elkhart - Mount Enterprise fault system, which is located in the southern part of the study area and has a mean strike of 060° (fig. 2), has exerted little perturbation on the regional vector pattern.

Vector Summation of Greater-Than-Average Peaks

The pairs of vector sums for each northwest and northeast quadrant represent an objective method of deducing general trends. However, vector sums are insensitive to the presence of more than one peak in each quadrant, or to local variations that might be produced by salt diapirism and regional faulting. Accordingly, vectors were also determined for individual greater-than-average peaks in 15-minute quadrangles (fig. 16). These peaks are defined as a sector or group of adjacent sectors having a relative magnitude greater than the arithmetic mean ($\bar{x} = 1/18 = 0.0\bar{5}$). Where a greater-than-average peak is bimodal, each of the two peaks was tested against the mean of the entire peak using the χ^2 one-sample test to determine whether the bimodal distribution is significant. If both peaks were found to be significantly different from the mean, then each was regarded as being an individual peak. Peaks with lower-than-average magnitudes (less than $0.0\bar{5}$) are not considered

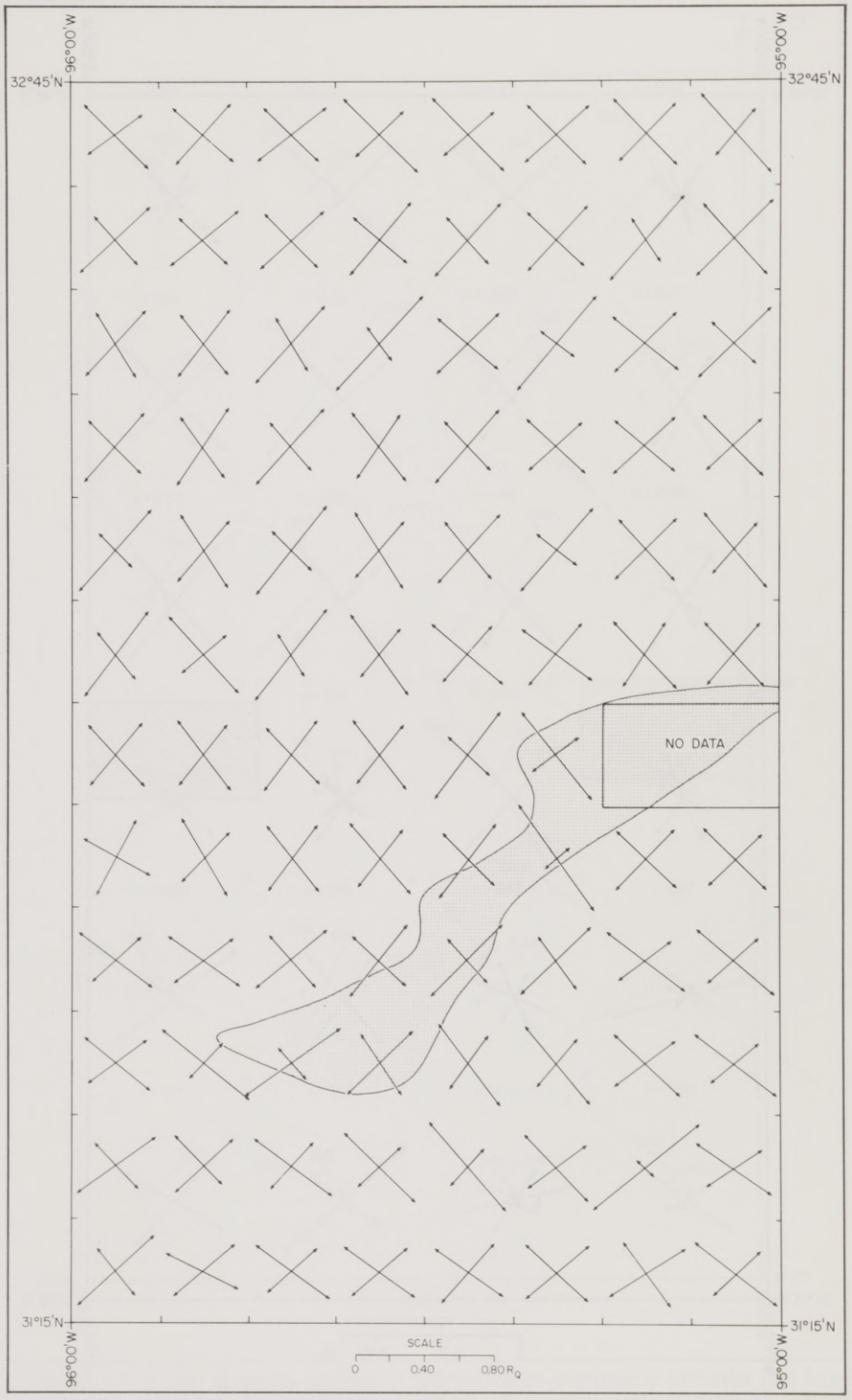

Figure 15. Polar graphs showing vector sums (R_Q) for all lineaments in northeast-southwest and northwest-southeast quadrants in each 7.5-minute quadrangle in study area I. Stippled area indicates extent of Elkhart - Mount Enterprise fault zone.

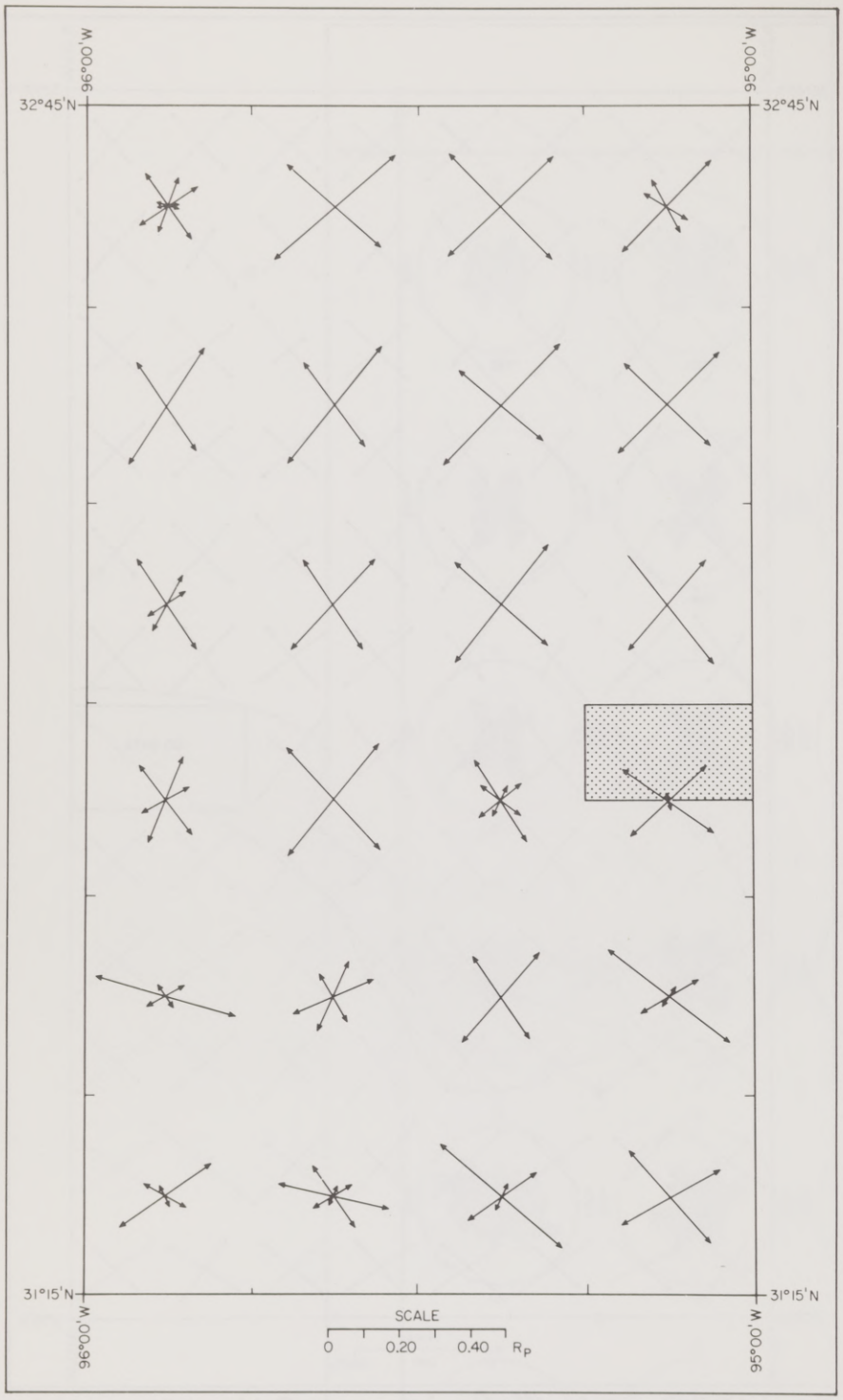

Figure 16. Polar graphs showing peak vector sums (R_P) for greater-than-average peaks in each 15-minute quadrangle in study area I. Photographic coverage in stippled area was unavailable.

significant. Because the number of lineaments in 7.5-minute quadrangles (mean frequency equals 88) was not considered sufficiently large for meaningful statistical analysis (see p. 12), the lineament data were combined to give twenty-four 15-minute quadrangles (mean frequency equals 345).

Sixty-four greater-than-average peaks are present in the twenty-four 15-minute quadrangles. Trends within the northern half of the area are more consistent than are those in the south.

χ^2 Test of Significance

All greater-than-average peaks are not necessarily significant because these can be generated purely randomly, as shown in a previous section. To exclude peaks having no geologic significance, a statistical test was applied. Two different approaches have been used in the past to test orientation data:

(a) Peaks can be tested to determine whether they depart significantly from a uniform distribution represented by the arithmetic mean (Offield, 1975). Either parametric (assuming a Von Mises, or circular-normal, distribution) or nonparametric tests can be applied;

(b) Each peak can be tested individually, regardless of its size, and without reference to the mean value (Frost, 1977).

For this study, the first method was used because peaks with magnitudes less than the mean are considered to have resulted purely from a deficiency of lineaments in adjacent sectors, rather than from an abundance of lineaments in the sectors forming the peaks. The mean value represents the distribution of an infinite number of randomly oriented lineaments; for a peak to be significant, therefore, its magnitude must be greater than the mean.

Because a circular-normal distribution cannot be assumed, the χ^2 one-sample nonparametric test was applied (Siegel, 1956, p. 42-47; Vistelius, 1966, p. 47-48). This test requires the use of lineament frequency, rather than magnitude. To accommodate this requirement, the length-weighted frequencies were used (F in table 1). Fifty-one of the 64 greater-than-average peaks in figure 16 were found to be significant at the 95-percent

confidence level. At the 99-percent confidence level, 45 peaks are significant. By dividing the X^2 value for each peak by the degrees of freedom (ν = k-1, where k equals the number of 10° sectors forming the peak), the Bernshtein accuracy criterion, H, was determined (Vistelius, 1966, p. 53-54). The values for each peak were then plotted as a Bernshtein vector with magnitude H and orientation equal to that of the vector sum obtained earlier (fig. 17).

It is obvious that almost the entire study area is characterized by statistically significant lineament peaks oriented approximately northwest and northeast. Subtle fluctuations in orientation as well as variable numbers of significant peaks are also present. Because the length of each of the H vectors in figure 17 is proportional to the significance of the lineament peak, these vectors provide an objective means of assessing the significance of subtle variations in orientation. If the H values in each 5° sector are summed, evidence is clear for the existence of bimodal populations in each 90° sector; that is, there are two northeast peaks at 045° and 055° and two northwest peaks at 310° and 325°, respectively (fig. 18). Although the orientation data were originally grouped in 10° sectors (for example, fig. 13), 5° sectors were selected for summation of the H values in figure 18 in order to accommodate the mean between adjacent 10° sectors. These four peaks may be grouped into two orthogonal pairs, but in view of the surprisingly common occurrence of this by purely random ordering (table 2), we do not regard this as particularly significant.

Recognition of these four lineament peaks provides a means of dividing the area into domains of similar preferred orientation. Division on the basis of the two northeasterly peaks (fig. 19) indicates a well-defined Domain A_1, characterized by the 045° peak,

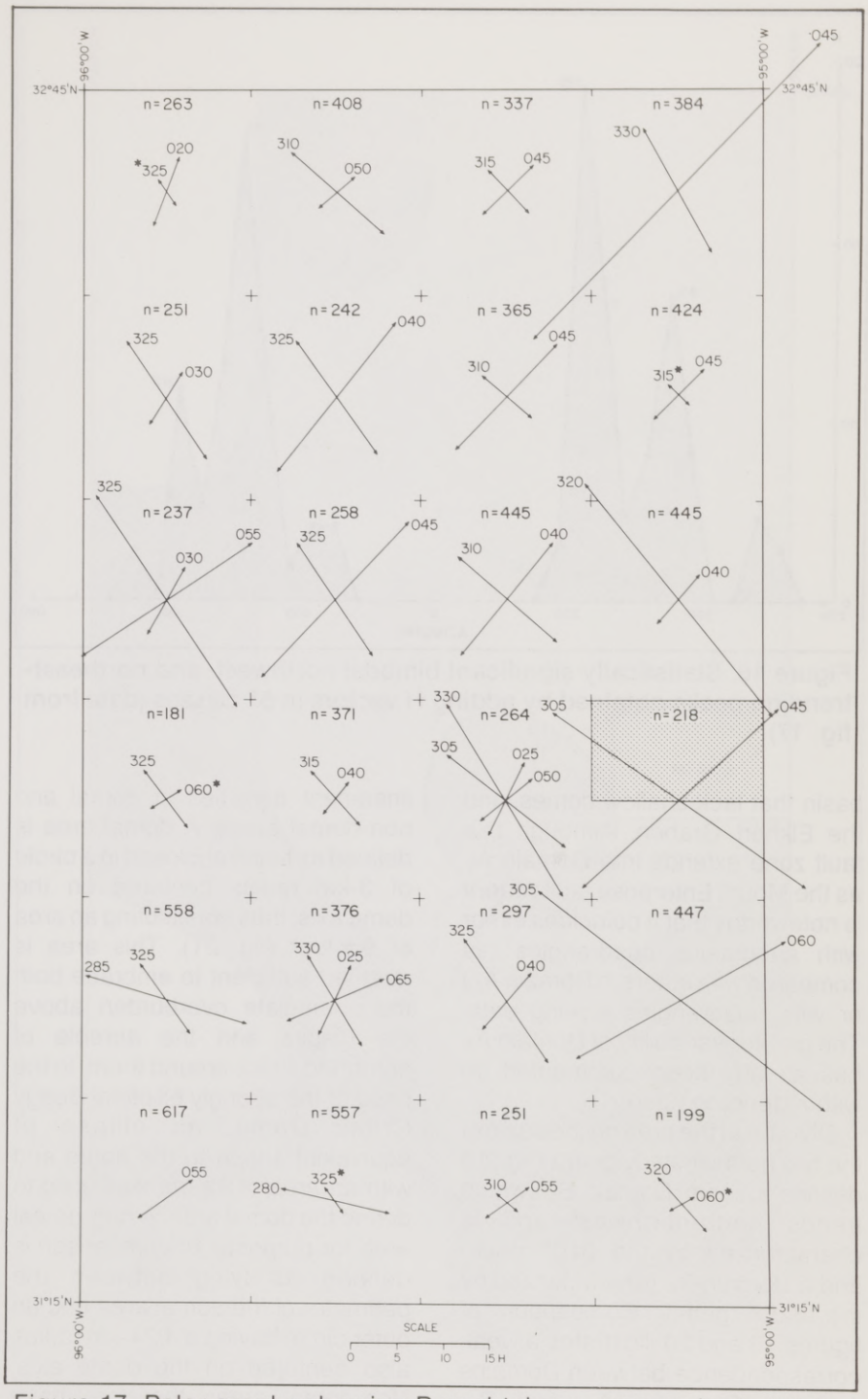

Figure 17. Polar graphs showing Bernshtein accuracy criteria (H) for greater-than-average peaks in each 15-minute quadrangle of study area I. Photographic coverage in stippled area was unavailable. Vector lengths are proportional to significance of preferred orientations. Asterisks denote peaks significant at 95-percent level only; all other peaks also significant at 99-percent level.

which is fringed by a less continuous Domain A_2 characterized by the 055° peak. Domain A_1 contains most of the shallow salt domes including all of the northern shallow salt domes. Domain A_2 contains the southernmost salt domes, the eastern parts of the

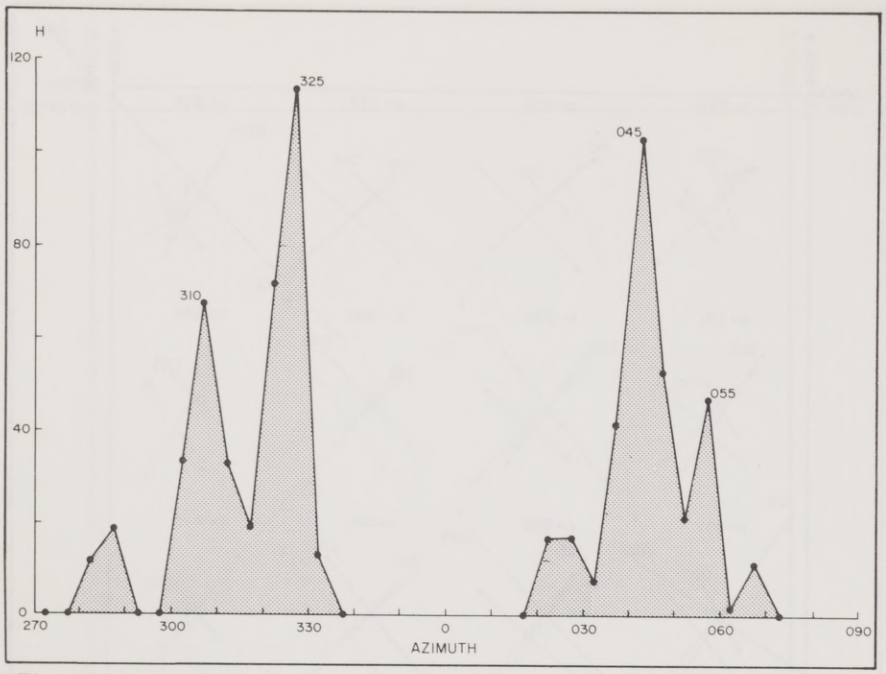

Figure 18. Statistically significant bimodal northwest- and northeast-trending peaks obtained by adding H vectors in 5° classes (data from fig. 17).

basin that lack shallow domes, and the Elkhart Graben. Although this fault zone extends into Domain A_1 as the Mount Enterprise fault zone, it is noteworthy that it coincides either with anomalous quadrangles (as compared with others in Domain A_1) or with quadrangles lacking data. The greater variability of Domain A_2 has already been commented on with respect to figure 16.

Division of the area on the basis of the two northwesterly peaks (fig. 20) defines a linear Domain B_1 (which trends north-northwest and is characterized by the 310° peak) and a Domain B_2 (characterized by the 325° peak). Comparison of figures 19 and 20 illustrates a weak correspondence between Domains A_1 and B_1, and A_2 and B_2, respectively. However, there appears to be no geologic explanation for subtle differences between Domains B_1 and B_2.

Effect of Diapirs on Lineament Density

The relation between lineament density and proximity to diapirs can be investigated by comparing lineament densities in domal and non-domal areas. A domal area is defined as being enclosed in a circle of 3-km radius centered on the dome axis, thus constituting an area of 9π km^2 (fig. 21). This area is deemed sufficient to embrace both the immediate overburden above the diapirs and the aureole of deformed strata around them. In the case of the strongly elliptical Boggy Creek Dome, an ellipse of equivalent shape to the dome and with an area of 9π km^2 was used to define the domal area. A non-domal area for purposes of comparison is defined as lying between the perimeter of the domal area and an outer circle having a 4.24-km radius also centered on the dome axis. Non-domal areas therefore have the same area as the domal areas but in each case completely enclose them.

Lineament densities were measured for each of the 13 domal areas and equivalent non-domal areas around salt domes situated at less than 1,000 m depth. In the case of a lineament crossing the boundary between the domal and non-domal areas, the actual length of the lineament in each area was used in the calculation. The southern domes have a significantly higher lineament density than the northern domes (fig. 22 and table 4). Although our data suggest that southern domal areas contain more lineaments than do southern non-domal areas (fig. 22), this is not statistically substantiated (table 4). Domal areas and non-domal areas do not have different overburden lithologies, so the higher densities of the southern domes cannot be ascribed to lithologic control. This conclusion also holds when comparing lineament densities in non-domal areas in the north and south; the similarity confirms a lack of lithologic control.

Effect of Diapirs on Degree of Preferred Orientation

If salt structures have influenced lineament trends by perturbation of the regional structure, their radial and concentric fracture patterns should increase the diversity of lineament trends as well as the density of lineaments. To test this hypothesis, the degree of preferred orientation was determined for each 7.5-minute quadrangle. The IPO value (table 1) can theoretically range from 0 percent (completely uniform distribution) to 100 percent (perfect unimodal distribution). A plot of IPO values against depth to salt or cap rock for each dome (fig. 23) reveals a tendency for shallow domes to be associated with lower degrees of preferred orientation than deeper domes. In the case of the 13 domes situated at depths of less than 1,000 m, there is a positive correlation at the 99-percent confidence level ($r = +0.743$); this is consistent with the above hypothesis that shallow domes have a greater effect on the regional lineament pattern than do deeper domes. The domes displaying the lowest degrees of preferred orientation are Oakwood, Keechi,

Palestine, and Butler (fig. 23). This suggests that southern domes have had a greater influence on both lineament density and degree of preferred orientation of lineaments than have the northern domes.

RESULTS OF THE LANDSAT STUDY

Lineament data in the Landsat study were processed according to the procedures described previously. The study area was divided into four subareas of approximately equal extent (fig. 24). Subarea C corresponds to the aerial photographic study area I. Polar graphs and Bernshtein values are given in figures 25 and 26. Of the 17 peaks tested statistically, eight are significant at both the 95-percent and 99-percent confidence levels. Because the number of lineaments in each subarea is small (ranging from 38 to 99), the confidence level should be very high if all randomly produced peaks are to be excluded.

Subarea A, which encompasses the Mexia-Talco fault system, contains three statistically significant peaks oriented at 315°, 005°, and 020°. The peak oriented at 315° corresponds to the northwest peak in subarea C, and in study area I. The peak at 005° probably reflects lithologic control because it is parallel to the contacts of stratigraphic units in the area. The peak oriented at 020° is parallel to mapped fault traces, although only one lineament corresponds spatially to a known fault trace.

Subareas B and D contain one and two significant peaks, respectively (fig. 26). The orientations of these peaks do not correspond to the Mexia-Talco fault system (in the case of subarea B), or other lineament maxima.

Subarea C corresponds closely to study area I and contains statistically significant peaks at 315° and 060°. As noted above, the former corresponds to the northwest peak in both subarea A and study area I. The 060° trend, however, lies 15° south of the northeast trend in study area I. This subarea, which corresponds to the salt dome province, contains the greatest number of lineament peaks. Only two of these peaks are statistically significant, but this greater diversity may well reflect increased radial and concentric fracturing induced by halokinesis, as suggested in the airphoto study.

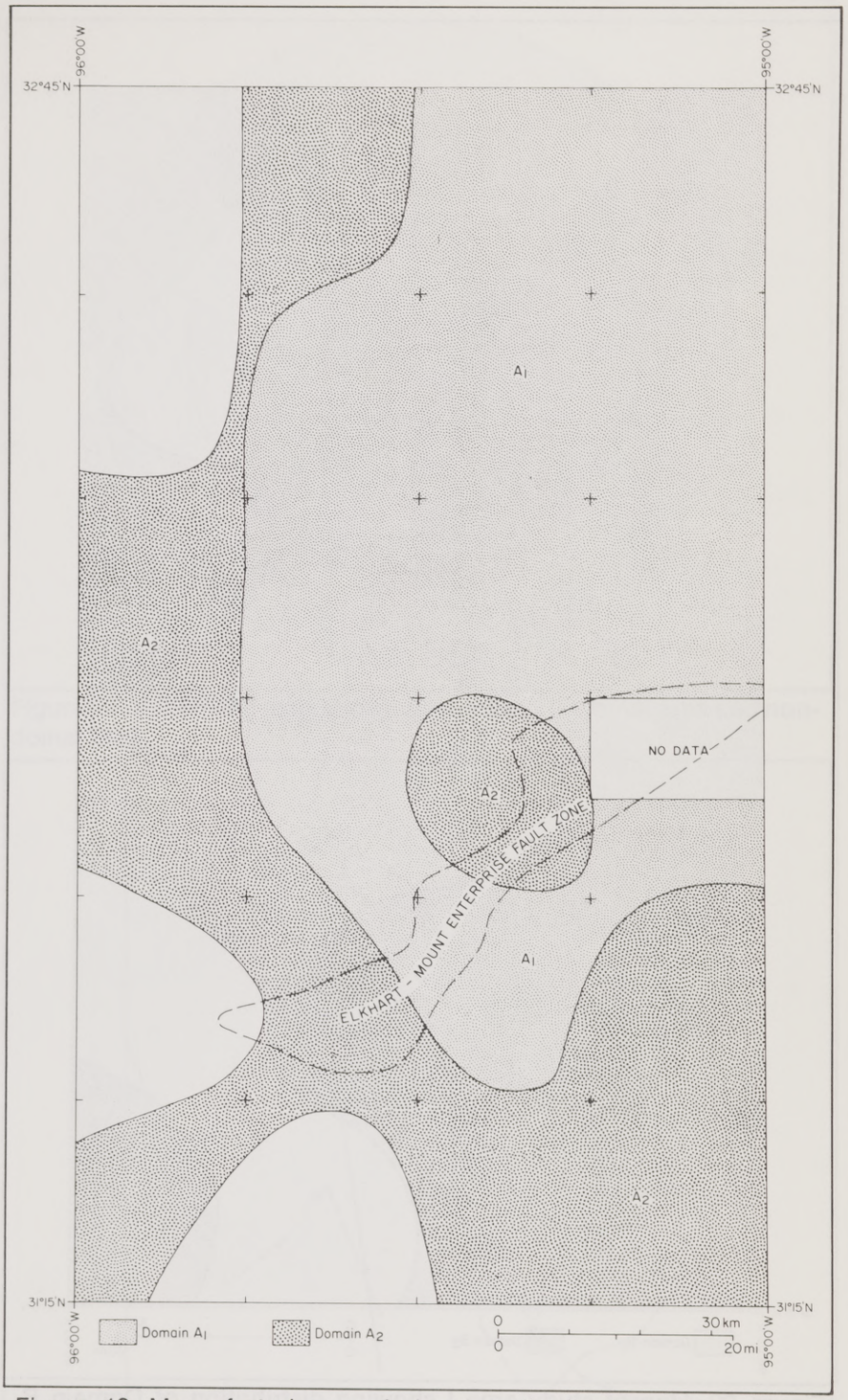

Figure 19. Map of study area I showing distribution of Domain A_1 (characterized by the 0.45° peak) and Domain A_2 (characterized by the 055° peak).

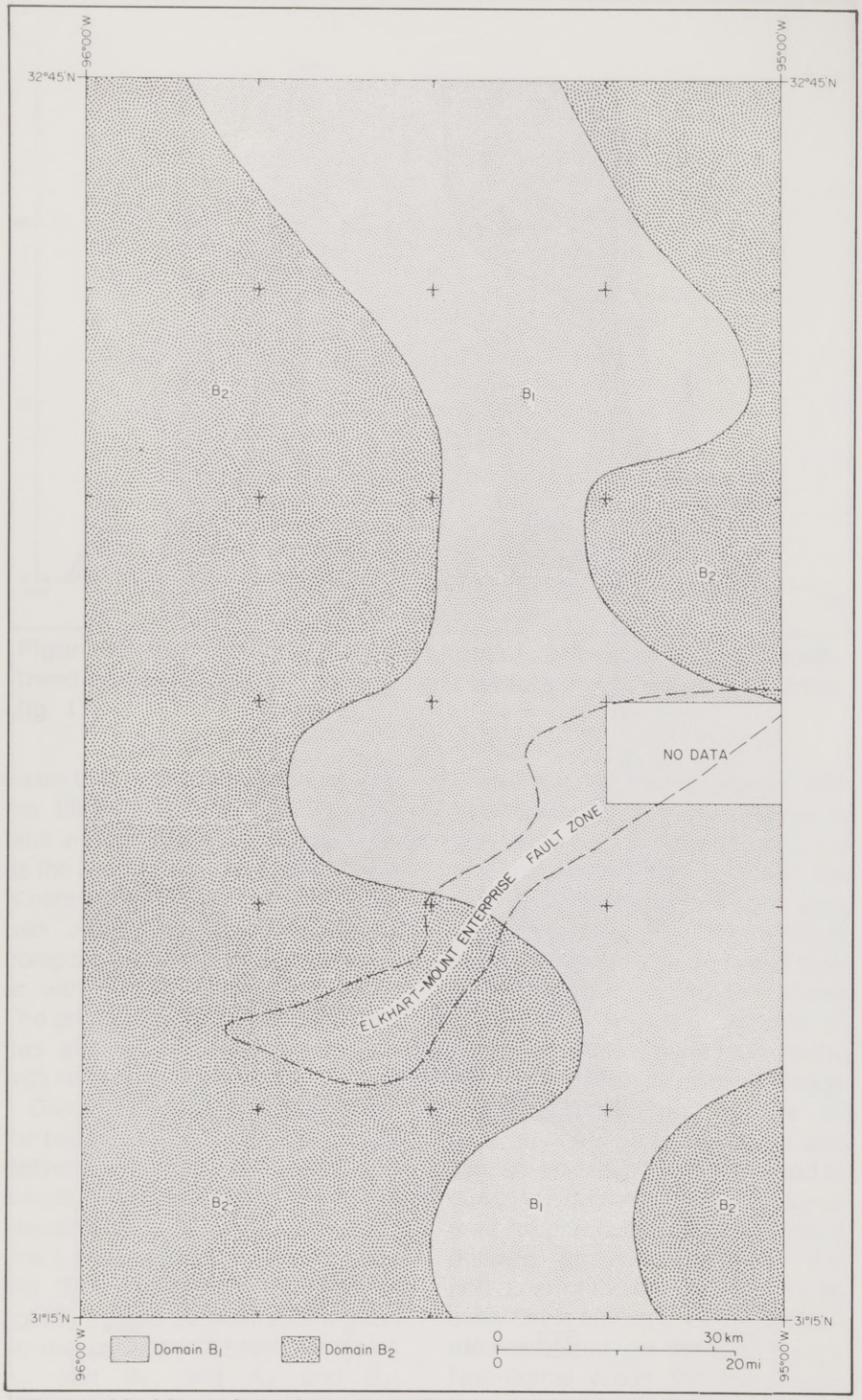

Figure 20. Map of study area I showing distribution of Domain B_1 (characterized by the 310° peak) and Domain B_2 (characterized by the 325° peak).

DISCUSSION

Lineaments have been identified in continental crust throughout the world from aerial photographs, Landsat, infrared, and radar imagery (for example, Hobbs, 1911; Rumsey, 1971; Offield, 1975; Frost, 1977; Sabins, 1978; Corbett, 1979). Linear anomalies on aeromagnetic maps have been identified in both continental crust (Frost, 1977) and oceanic crust, where they provide fundamental evidence for seafloor spreading (Corbett, 1979).

A high proportion of lineaments reported in the literature do not display obvious evidence of either horizontal or vertical displacement; they may represent zones of structural weakness (Johnson, 1976). Some are postulated to have formed in the Precambrian basement and to have subsequently propagated up through younger strata in response to rejuvenation or differential compaction of cover over uneven basement (Rumsey, 1971; Haman and Jurgens, 1976; Corbett, 1979). Lineament trends in cover have been found to correlate well with trends in the underlying basement (Lattman and Nickelsen, 1958; Frost, 1977). This is compatible with the hypothesis of upward propagation of lineaments from underlying bedrock.

Lineaments and Regional Faults

The two regional lineament trends established from the East Texas aerial photographic study (315° to 330°, and 035° to 050°) correlate well with lineament, fault, and fracture patterns in Louisiana and the Gulf Coast Plain in general (Wermund, 1955; Murray, 1961, p. 85-88; Saunders, 1979, fig. 1). Figures 19 and 20 demonstrate that although there is a bimodal distribution of lineaments in each 90° sector in the area as a whole, these double peaks are mutually exclusive. Accordingly, one domain is characterized by, for example, a peak oriented toward 045°, whereas an adjoining domain contains a peak trending 055°. The 045° trend, which is dominant in the central and northeastern part (Domain A_1 in fig. 19), does not coincide with the trend or location of known fault traces at the surface (fig. 3). However, this trend is paralleled by subsurface faults

trending roughly 040° (fig. 2), which are particularly abundant in Domain A_1. Most of these faults represent grabens along the crests of subsurface anticlines, which are cored with either anomalously thick clastic units known as turtle structures, or salt. The 045° trend is also approximated in the residual gravity map of the same area (fig. 27). The linear gravity anomalies trend between 040° and 020°. Other studies in the East Texas Waste Isolation program have shown that the positive and negative gravity anomalies generally correspond to zones where salt is absent or present, respectively. The trends of gravity anomalies and subsurface faults therefore show a close correlation. The reason for a similar correlation with preferred orientation directions of lineaments in Domain A_1 is less clear. It is debatable whether this parallel alignment is fortuitous or connected in some way; if connected, it may be that subsurface faulting is expressed as surface fracturing without mappable displacements or that these faults extend to the surface but have not been recognized because of the poor outcrop characteristic of East Texas.

The 055°-trending lineament peaks, which are common in the western and southern parts of the study area, are approximately parallel to the Elkhart - Mount Enterprise fault zone, which is also broadly reflected by linear anomalies of residual gravity (fig. 27). The fact that the fault zone is not spatially associated with any dramatic perturbation of the regional lineament pattern can be ascribed to several factors: (1) the fault zone is approximately parallel to one of the regionally developed lineament peaks and is therefore masked; (2) one of the three 15-minute quadrangles containing the fault zone is partly lacking in data (fig. 17); (3) the 15-minute quadrangles may be too large to reflect the influence of a fault zone

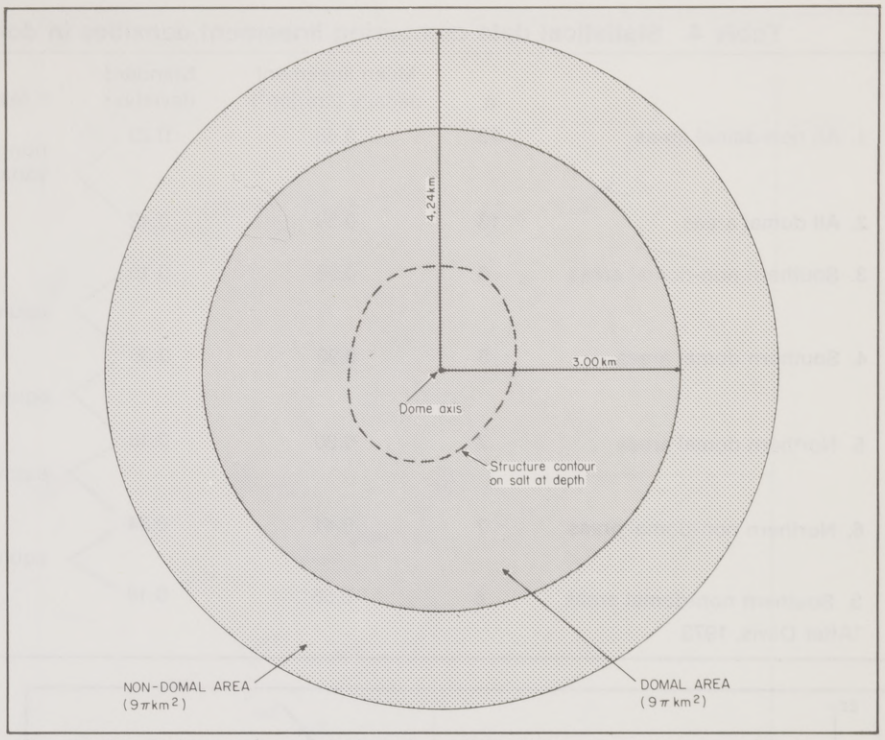

Figure 21. Schematic map showing definition of domal area and non-domal area.

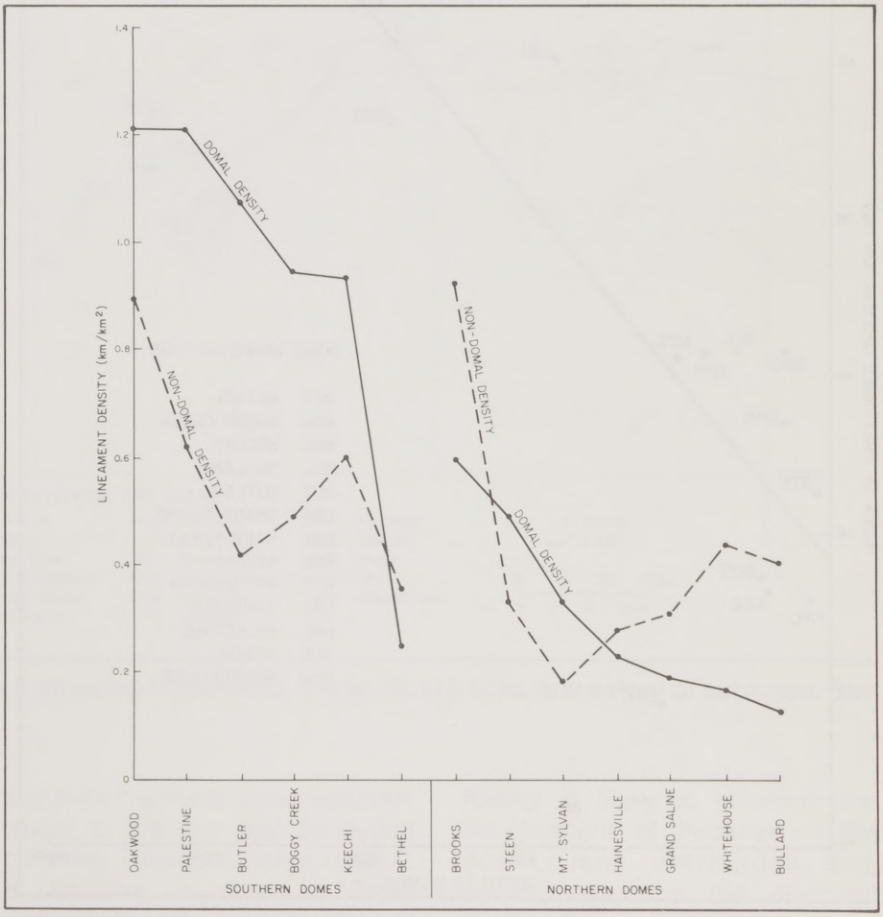

Figure 22. Graph of lineament densities in domal areas and non-domal areas for all 13 domes less than 1,000 m deep in study area I.

Table 4. Statistical data comparing lineament densities in domal and non-domal areas.

	n	Mean lineament density (km/km^2)	Standard deviation	F test* (95% level)	t test* (95% level)
1. All non-domal areas	13	0.48	0.23	nonequivalent variances	invalid
2. All domal areas	13	0.59	0.42		
3. Southern non-domal areas	6	0.56	0.19	equivalent variances	no significant difference in means
4. Southern domal areas	6	0.93	0.36	equivalent variances	significant difference in means
5. Northern domal areas	7	0.30	0.18	equivalent variances	no significant difference in means
6. Northern non-domal areas	7	0.41	0.24	equivalent variances	no significant difference in means
3. Southern non-domal areas	6	0.56	0.19		

*After Davis, 1973

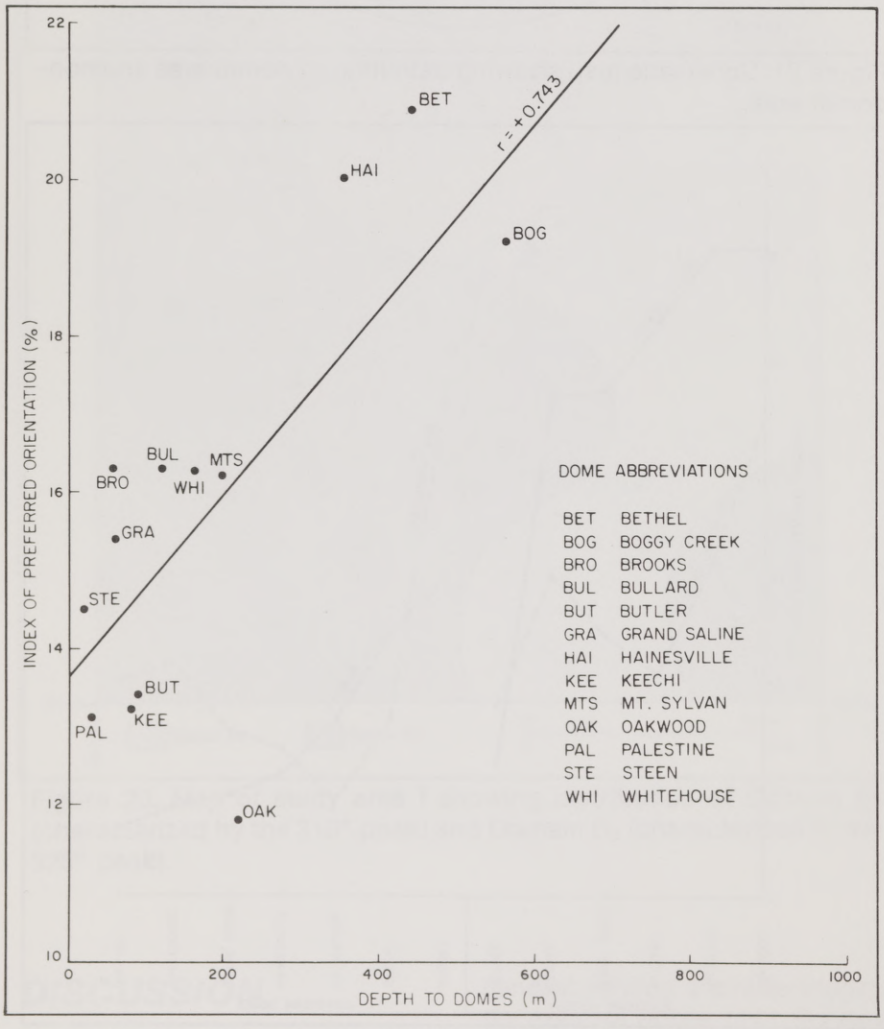

Figure 23. Graph showing correlation (at 99-percent confidence level) between depth to domes and index of preferred orientation (IPO) for 7.5-minute quadrangles containing shallow domes in study area I.

extending across them. Factor 3 is partly negated by the fact that the more sensitive 7.5-minute quadrangles are also devoid of anomalies attributable to the fault zone (fig. 15).

Is there an explanation for the fact that the southern area (Domain A_2 in fig. 19) contains a northeasterly peak subtly different from the area farther north? It is tempting to ascribe this preferred orientation to the Elkhart - Mount Enterprise fault zone crossing this area. However, there are a number of reasons that this explanation should be treated with caution: (1) few lineaments in the study area spatially correspond to mapped faults; (2) the fault zone is not reflected in an increased number of lineaments (fig. 14); (3) the lineament peaks in the two quadrangles covering the Elkhart - Mount Enterprise fault zone are about 20° oblique to the trend of fault traces; (4) similar lineament trends are present in the western part of the basin, tens of kilometers north of the fault zone (fig. 19); and (5) the very marked northwesterly lineament peaks are certainly unrelated to faulting. It may therefore be concluded that whereas the Elkhart-Mount Enterprise fault zone is spatially associated with subtle variations in the regional lineament

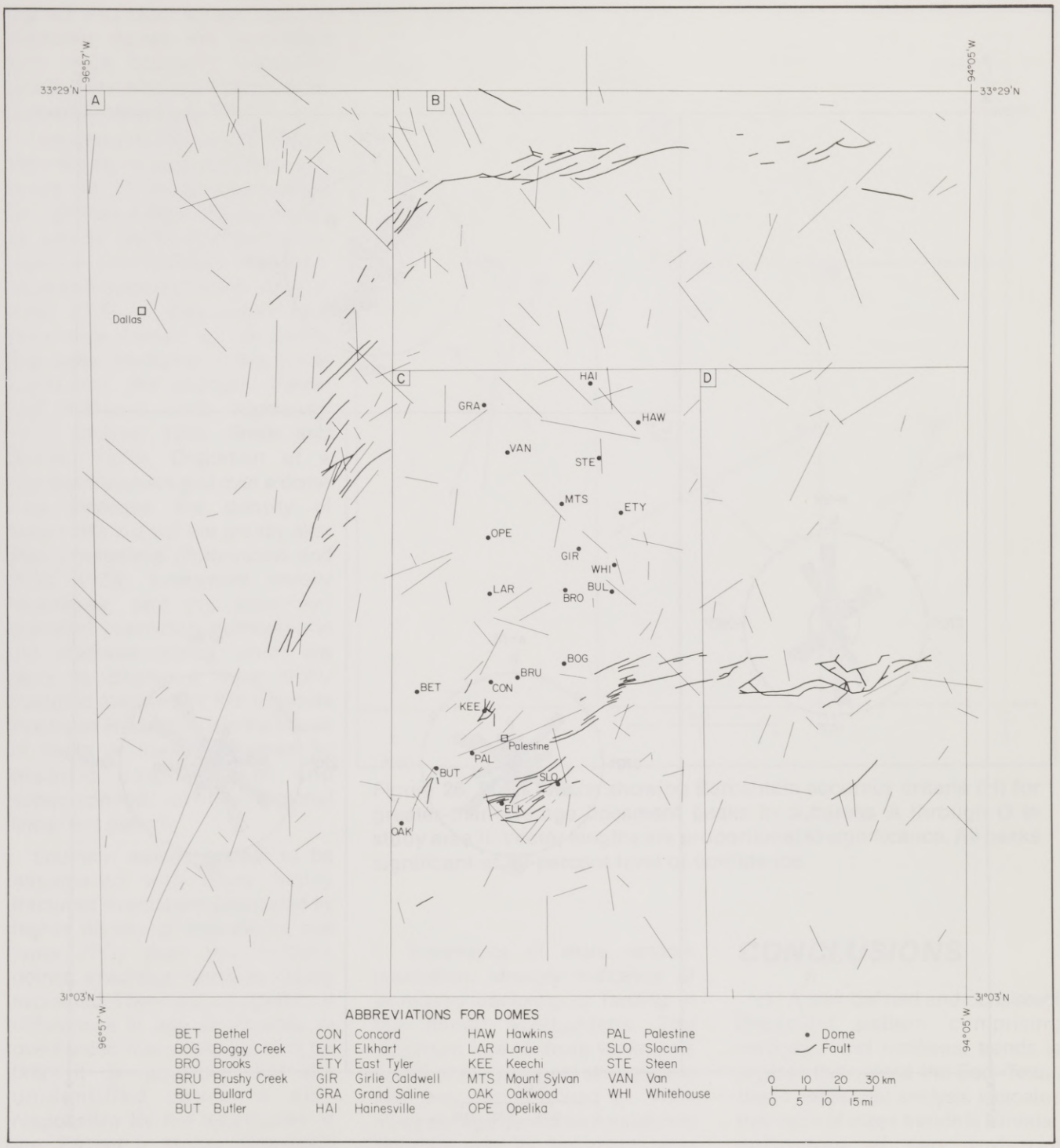

Figure 24. Map of Landsat study area II showing lineaments, known fault traces, and extent of subareas. See figure 1 for location.

pattern, there is no statistically significant evidence that the variations in lineament preferred orientation are a reflection of this fault zone. Gravity data indicate variations in the trend of salt structures at depth (fig. 27); this suggests that the lineament pattern, which is strikingly well developed but subtly varied over large areas, is a reflection of folding at depth caused by the mobilization of Louann Salt into salt-cored anticlines, domes, and diapirs. This folding is likely to influence the development of fractures in the post-Louann overburden and, hence, influence the drainage pattern that defines such a large proportion of the lineaments recognized in this study.

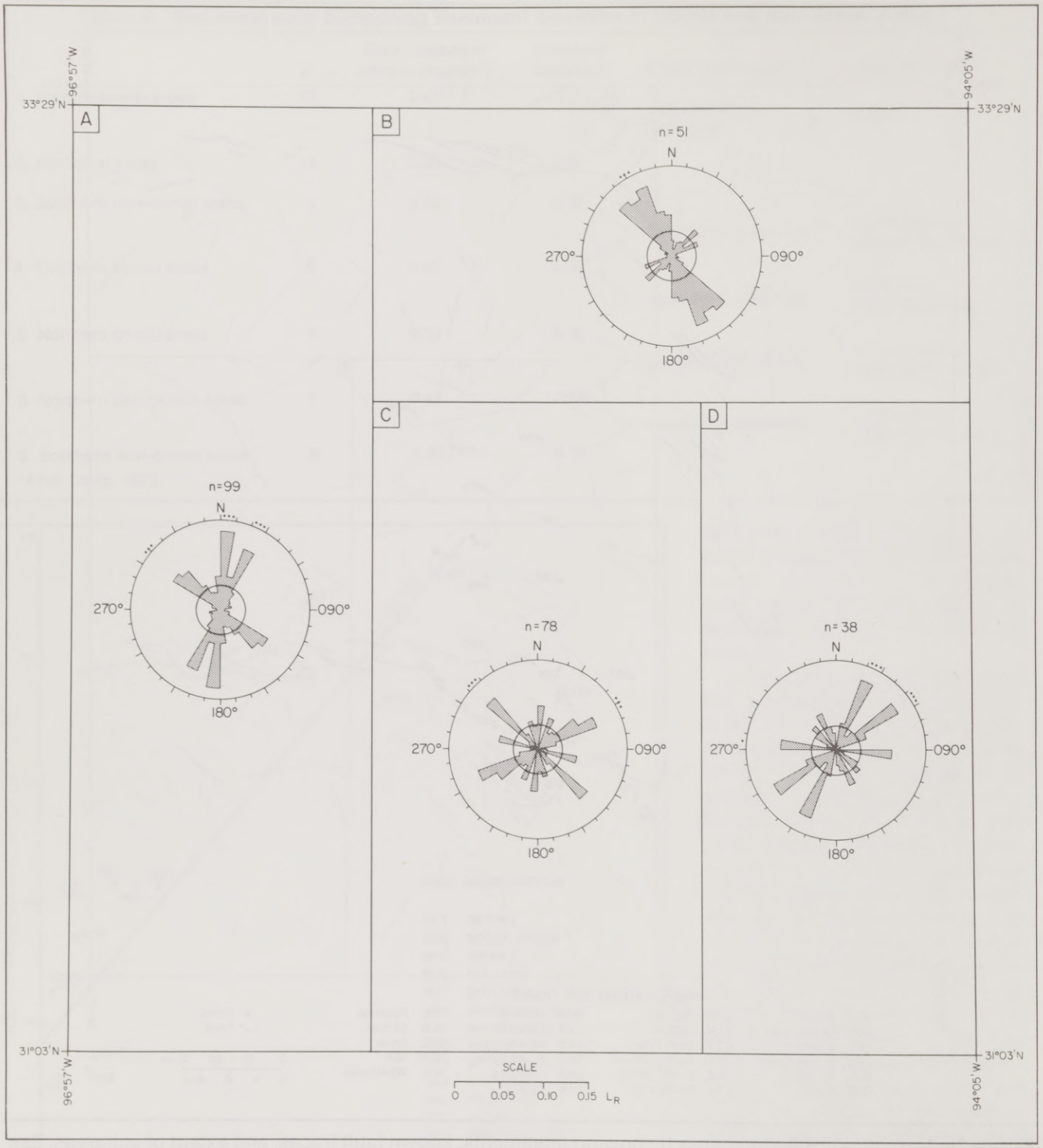

Figure 25. Polar graphs showing relative lengths (L_R) of Landsat lineaments in subareas A through D in study area II. Significance levels of peaks: one dot, 90 percent; two dots, 95 percent; three dots, 99 percent. Inner circle represents arithmetic mean.

Lineaments and Salt Domes

The nine western 15-minute quadrangles in the southern subarea have the lowest H values, indicating peaks with low levels of statistical significance (fig. 17). This area corresponds to a high concentration of salt domes, four of which (Oakwood, Palestine, Keechi, and Butler) have the lowest IPO values, indicating high degrees of lineament dispersion. It has been established that the southern domes are associated with a significantly greater density of lineaments than the northern domes

(fig. 22 and table 4) and that the shallower domes are associated with more scattered lineament orientations reflected in significantly lower IPO values (fig. 23).

The apparent influence of shallow salt domes on regional lineament trends (fig. 23) could be accounted for in two ways. Either the domes act as circular uplifts that distort the regional, approximately orthogonal lineament pattern (Podwysocki and Gold, 1979), or they create new lineaments formed by concentric and radial fracturing in the domal overburden (for example, Parker and McDowell, 1955; Hightower, 1958; Murray, 1966; Smith and Reeve, 1970). Distortion of a regional lineament grid over a dome may increase the density of lineaments but will not greatly alter their orientations (Podwysocki and Gold, 1979). Lineament density increases, and the lineament preferred orientation decreases in the shallower domes, which are likely to display a more highly fractured overburden; this suggests that these lineaments are the traces of faults or fractures formed by diapiric emplacement and superimposed on the regional lineament pattern.

Southern domes appear to be associated with more highly fractured overburden (indicated by higher density of lineaments and lower IPO) than the northern domes, a fact that cannot be readily explained. There are no significant differences in age or lithology of overburden that could account for this. It is possible that the unidentified cause is also responsible for the localization of the Elkhart - Mount Enterprise array of faults in the south because faults of similar orientation are scattered throughout the East Texas Basin.

One purpose of this investigation was to determine if the regional lineament pattern was suggestive of Holocene halokinesis. Results have shown that the southern salt domes are associated with higher densities of lineaments of more random orientation, strongly indicative of increased fracturing or faulting in the domal overburdens. The maximum age of these lineaments is that of the youngest stratigraphic unit they have formed in. Their minimum age cannot be established because, although lineaments have propagated upward from bedrock into modern drainage systems and surficial deposits, this propagation provides no clue to the age of the deformational event responsible for their structural control. Accordingly, this study has not been able to confirm or deny the occurrence of Holocene deformation in the East Texas Basin.

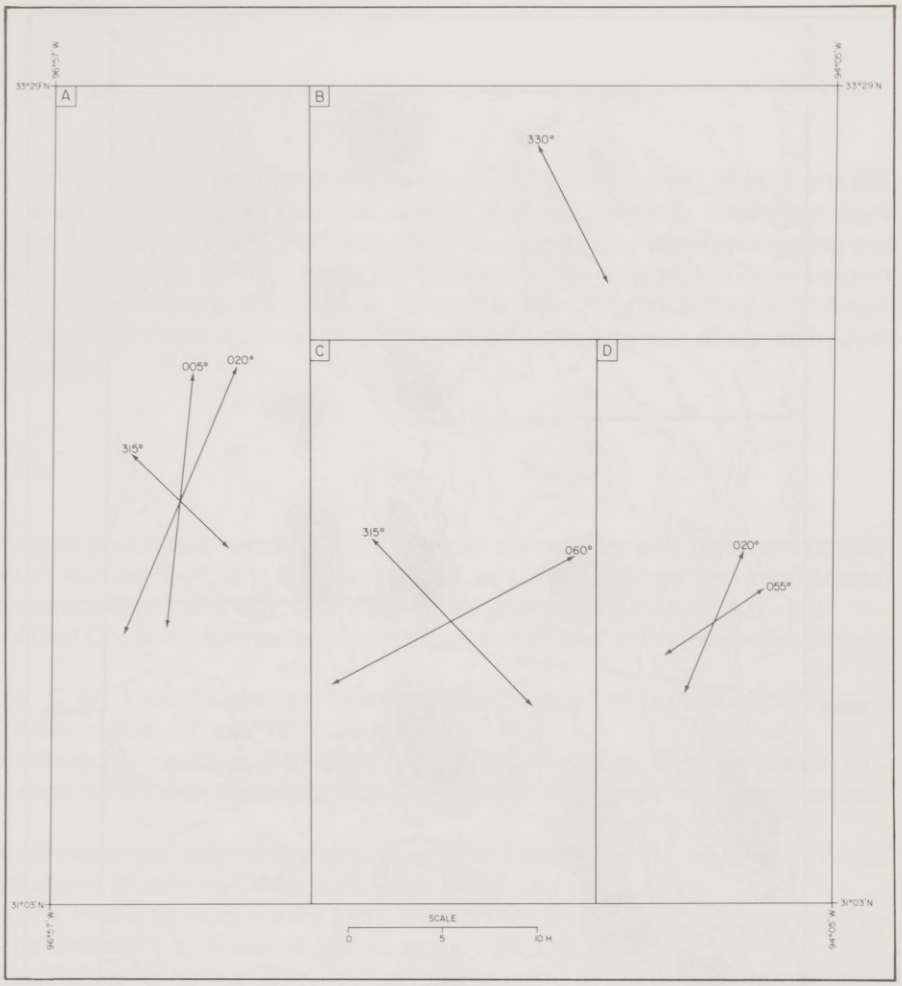

Figure 26. Polar graphs showing Bernshtein accuracy criteria (H) for greater-than-average lineament peaks in subareas A through D in study area II. Vector lengths are proportional to significance. All peaks significant at 99-percent level of confidence.

CONCLUSIONS

(1) A well-defined and consistent lineament pattern comprising northwest and northeast trends is present throughout the East Texas Basin. Statistical analysis indicates that each of these trends is bimodal, consisting of two preferred orientations 15° to 20° apart. Study area I may be divided into structural domains on the basis of the dominance of each component of the bimodal peak.

(2) The northeast-trending set of lineaments is parallel to the individual faults making up the Mexia-Talco array, to subsurface faults in the center of the basin, and,

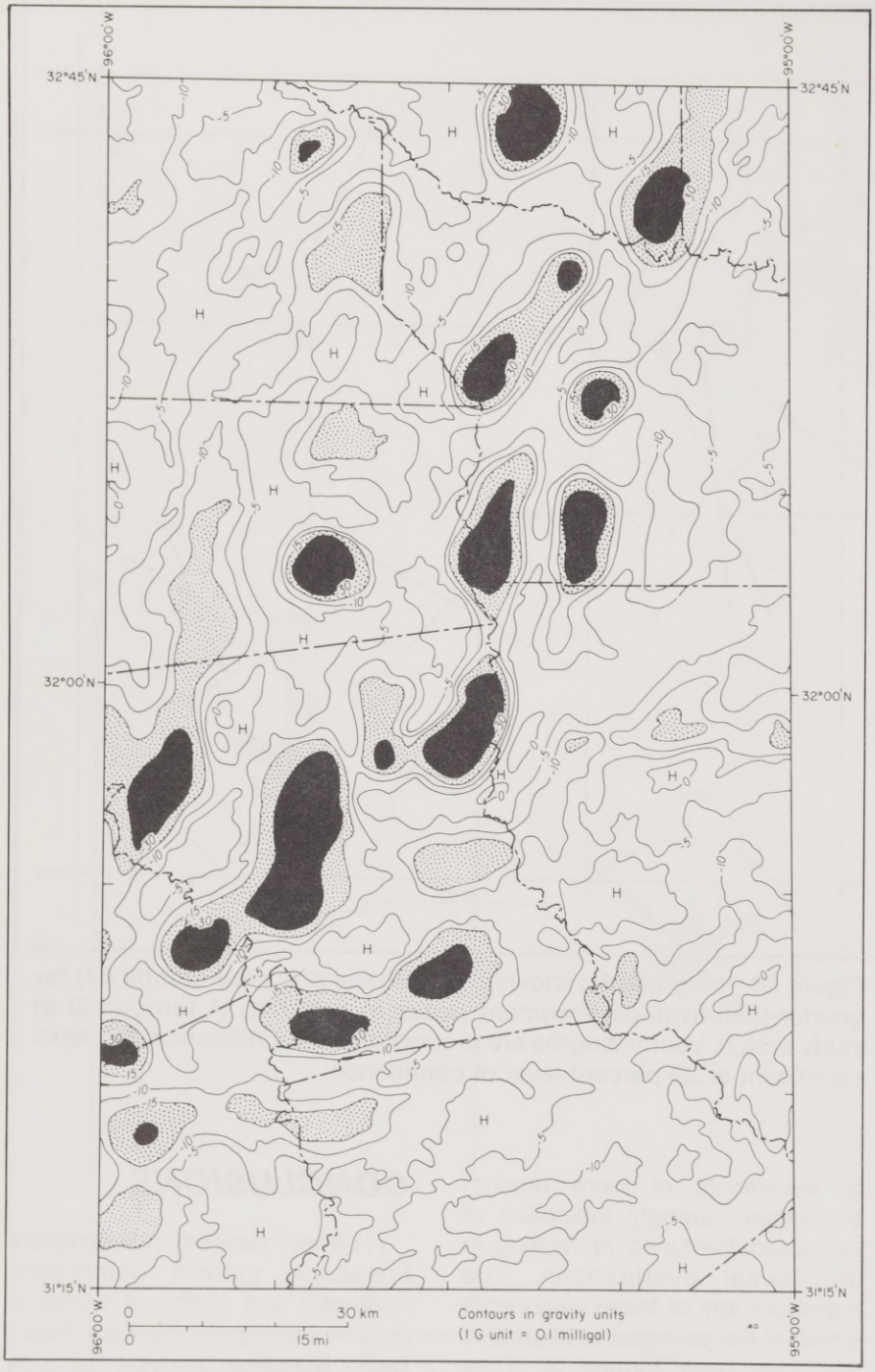

Figure 27. Map of residual gravity field in study area I. Black areas have less than -30 G units; H marks relative gravity highs. Data simplified from maps by Exploration Techniques, Inc. (1974).

in some places, to lithologic contacts.

(3) The northwest-trending set of lineaments is apparently not related to any particular structural element of the basin, but, like the northeast-trending set, is thought to reflect preferential directions of fracture induced by interference folding at depth caused by halokinesis and reflected in the regional gravity field.

(4) Shallow domes in the south have had a significant influence on the regional lineament pattern by increasing the dispersion in orientation of the lineaments and by increasing their density. Fracturing and faulting of domal overburden is a probable cause.

(5) The Elkhart - Mount Enterprise fault zone has had little effect on the regional lineament pattern; this is partly because a lack of data in part of the zone obscures this effect and partly because individual faults constituting the fault zone are parallel to the regional pattern. A number of reasons suggest that regionally developed fracturing, rather than the fault zone itself, is likely to be the main cause of the lineament pattern.

(6) Because most of the lineaments are defined by straight segments of drainage channels, their recognition has been only weakly hampered by cultivation. However, areas covered by flood-plain deposits have significantly fewer lineaments.

(7) Although the scale of the aerial photographs varies from 1:17,400 to 1:25,500, no relation between scale and numbers of lineaments recorded was proven.

(8) The size of lineament peaks is more a function of lineament frequency than of lineament length.

(9) The peak vector sum provides the most precise representation of the azimuth of preferred orientation. The Bernshtein accuracy criterion serves as a statistical measure of the degree of significance of this azimuth.

(10) Study of lineament distributions generated artificially by random processes indicates that orthogonal sets are almost invariably present, and suggests that the geologic significance of orthogonal pairsets has been exaggerated in the literature.

(11) The artificial data sets also show that confidence levels of 90 percent or 95 percent, commonly employed in the literature, are insufficiently rigorous to reject non-significant peaks formed by random ordering; a confidence level of 99 percent is required, particularly if the samples contain fewer than 200 lineaments.

ACKNOWLEDGMENTS

This work was funded by the U.S. Department of Energy under contract numbers DE-AC97-79ET-44605 and DE-AC97-80ET-46617. Data for this study were collected by Richard W. Debus and Jacqueline D. Smith. We thank reviewers R. J. Finley, A. G. Goldstein, and E. G. Wermund for their constructive suggestions. Word processing was done by Dorothy C. Johnson and Margaret T. Chastain, with typesetting by Charlotte J. Frere, under the supervision of Lucille C. Harrell. Editing was by Michelle C. Pemberton. Drafting was by Micheline Davis, Margaret Day, John Ames, David Ridner, and Charlie Rogers, under the supervision of James W. Macon. This publication was designed by Judy P. Culwell and assembled by Jamie S. Haynes.

REFERENCES

Babcock, E. A., 1976, A statistical analysis of photolineaments and joints, terrain parameters and lineament density near Lethbridge, Alberta, *in* Hodgson, R. A., Gay, S. P., and Benjamins, J. Y., eds., Proceedings, first international conference on the new basement tectonics: Salt Lake City, The Utah Geological Association, p. 437-448.

Cloos, E., 1968, Experimental analysis of Gulf Coast fracture patterns: American Association of Petroleum Geologists Bulletin, v. 52, no. 3, p. 420-444.

Collins, E. W., Hobday, D. K., and Kreitler, C. W., 1980, Quaternary faulting in East Texas: The University of Texas at Austin, Bureau of Economic Geology Geological Circular 80-1, 20 p.

Corbett, M. K., 1979, Origin of pervasive orthogonal fracturing of the Earth's crust, *in* Podwysocki, M. H., and Earle, J. L., eds., Proceedings, second international conference on basement tectonics: Denver, Basement Tectonics Committee, Inc., p. 319-325.

Curray, J. R., 1956, The analysis of two-dimensional orientation data: Journal of Geology, v. 64, no. 2, p. 117-132.

Davis, J. C., 1973, Statistics and data analysis in geology: New York, John Wiley and Sons, 550 p.

Exploration Techniques Incorporated, 1974, Profile residual gravity map: Unpublished proprietary data purchased by the Bureau of Economic Geology, The University of Texas at Austin, scale 1:96,000.

Fisher, R. A., and Yates, F., 1963, Statistical tables for biological, agricultural, and medical research: Edinburgh, Oliver and Boyd, 146 p.

Frost, R. T. C., 1977, Tectonic patterns in the Danish region (as deduced from a comparative analysis of magnetic, Landsat, bathymetric and gravity lineaments): Geologie en Mijnbouw, v. 56, no. 4, p. 351-362.

Gay, S. P., 1973, Pervasive orthogonal fracturing in Earth's continental crust: Utah, American Stereo Map Company, 124 p.

_____ 1976, Short note: standardization of azimuthal presentations, *in* Hodgson, R. A., Gay, S. P., and Benjamins, J. Y., eds., Proceedings, first international conference on the new basement tectonics: Salt Lake City, The Utah Geological Association, p. 499-500.

Gellert, W., Kustner, H., Hellwich, M., and Kastner, H., 1977, The VNR concise encyclopedia of mathematics: New York, Van Nostrand Reinhold Company, 760 p.

Geomap Company, 1979, Exploration summary of East Texas: Dallas, scale 1:316,800.

Haman, P. J., 1975, Discussion of "Photolineaments and regional joints: lineament density and terrain parameters, south central Alberta, by E. A. Babcock": Canadian Petroleum Geology Bulletin, v. 23, no. 4, p. 853-857.

Haman, P. J., and Jurgens, K., 1976, The discovery of the Caroline arch, Alberta, by lineament analysis, *in* Hodgson, R. A., Gay, S. P., and Benjamins, J. Y., eds., Proceedings, first international conference on the new basement tectonics: Salt Lake City, The Utah Geological Association, p. 153-162.

Hast, N., 1973, The existence of horizontal stress fields and orthogonal fracture systems in the Moon's crust: Modern Geology, v. 4, no. 2, p. 73-84.

Hightower, M. L., 1958, Structural geology of the Palestine Salt Dome, Anderson County, Texas: University of Texas, Austin, Master's thesis, 83 p.

Hobbs, W. H., 1911, Repeating patterns in the relief and in the structure of the land: Geological Society of America Bulletin, v. 22, no. 4, p. 123-176.

Johnson, A. C., 1976, Lineament analysis: an exploration method for the delineation of the structural and stratigraphic anomalies, *in* Hodgson, R. A., Gay, S. P., and Benjamins, J. Y., eds., Proceedings, first international conference on the new basement tectonics: Salt Lake City, The Utah Geological Association, p. 449-452.

Kvet, R., 1976, Planetary equidistant rupture (PER) systems in Moravia, Czechoslovakia, *in* Hodgson, R. A., Gay, S. P., and Benjamins, J. Y., eds., Proceedings, first international conference on the new basement tectonics: Salt Lake City, The Utah Geological Association, p. 290-294.

Lattman, L. H., and Nickelsen, R. P., 1958, Photogeologic fracture trace mapping in the Appalachian Plateau: American Association of Petroleum Geologists Bulletin, v. 42, no. 9, p. 2238-2245.

Murray, G. E., 1961, Geology of the Atlantic and Gulf Coastal province of North America: New York, Harper and Brothers, 692 p.

_____ 1966, Salt structures of Gulf of Mexico Basin — a review: American Association of Petroleum Geologists Bulletin, v. 50, no. 3, p. 439-478.

Offield, T. W., 1975, Thermal-infrared images as a basis for structure mapping, Front Range and adjacent plains in Colorado: Geological Society of America Bulletin, v. 86, no. 4, p. 495-502.

O'Leary, D. W., Friedman, J. D., and Pohn, H. A., 1976, Lineament, linear, lineation: some proposed new standards for old terms: Geological Society of America Bulletin, v. 87, no. 10, p. 1463-1469.

Parker, T. J., and McDowell, A. N., 1955, Model studies of salt-dome tectonics: American Association of Petroleum Geologists Bulletin, v. 39, no. 12, p. 2384-2470.

Pincus, H. J., 1956, Some vector and arithmetic operations of two-dimensional orientation variates, with applications to geological data: Journal of Geology, v. 64, no. 6, p. 533-558.

Plafker, G., 1964, Oriented lakes and lineaments of Northeast Bolivia: Geological Society of America Bulletin, v. 75, no. 6, p. 503-522.

Podwysocki, M. H., and Gold, D. P., 1979, Some possible surface expressions of a regular fracture grid deformed by subsurface structures, *in* Podwysocki, M. H., and Earle, J. L., eds., Proceedings, second international conference on basement tectonics: Denver, Basement Tectonics Committee, Inc., p. 542-559.

Reeves, J. R., 1976, Linears in Southeastern Alaska, *in* Hodgson, R. A., Gay, S. P., and Benjamins, J. Y., eds., Proceedings, first international conference on the new basement tectonics: Salt Lake City, The Utah Geological Association, p. 35-41.

Rumsey, I. A. P., 1971, Relationship of fractures in unconsolidated superficial deposits to those in the underlying bedrock: Modern Geology, v. 3, no. 1, p. 25-41.

Sabins, F. F., 1978, Remote sensing: Principles and interpretation: San Francisco, W. H. Freeman and Company, 426 p.

Saunders, D. F., 1979, Regional geomorphic lineaments on satellite imagery--their origin and applications, *in* Podwysocki, M. H., and Earle, J. L., eds., Proceedings, second international conference on basement tectonics: Denver, Basement Tectonic Committee, Inc., p. 326-352.

Siegel, S., 1956, Nonparametric statistics for the behavioral sciences: New York, McGraw-Hill, 312 p.

Smith, D. A., and Reeve, F. A. E., 1970, Salt piercement in shallow Gulf Coast salt structures: American Association of Petroleum Geologists Bulletin, v. 54, no. 7, p. 1271-1289.

Till, R., 1974, Statistical methods for the earth scientist: an introduction: New York, John Wiley and Sons, 154 p.

Vistelius, A. B., 1966, Structural diagrams: New York, Pergamon Press, 178 p.

Wermund, E. G., 1955, Fault patterns in northwest Louisiana: American Association of Petroleum Geologists Bulletin, v. 39, no. 11, p. 2329-2340.